Journal of
Materials Chemistry C

Materials for optical, magnetic and electronic devices

rsc.li/materials-c

ROYAL SOCIETY
OF **CHEMISTRY**

REVIEW ARTICLE
Enrica Soprano, Giulia Vanoni *et al*.
Advances in fluorescence-based point-of-care diagnostics:
probes, nanostructures and integrated systems

REVIEW

Check for updates

Advances in fluorescence-based point-of-care diagnostics: probes, nanostructures and integrated systems

Manuela Cedrún-Morales,*[ac] Enrica Soprano,[ac] Giulia Vanoni,[ac] Anil Chandra, [iD] [b]
Helena Iuele,[ac] Francesco Colella,[cd] Stefania Forciniti,[ac] Valentina Onesto,[ac]
Giuliana Grasso,[ac] Giuseppe Gigli[acd] and Loretta L. del Mercato [iD] *[ac]

Fluorescence-based point-of-care (POC) technologies are rapidly evolving through advances in materials chemistry. This review provides a comprehensive overview of fluorescent molecular probes, proteins, hybrid nanostructures, metal–organic frameworks, silica platforms, carbon dots, and upconverting nanoparticles engineered for portable diagnostics. We highlight fundamental photophysical mechanisms, design strategies for improving brightness, stability, and multiplexing, and the integration of fluorescent materials with microfluidics, wearable interfaces, and smartphone readouts. Current limitations, translational challenges, and emerging trends, including AI-enabled data analysis and next-generation NIR and AIE fluorophores, are discussed. Together, these insights outline how material innovation is driving the next generation of high-performance POC sensing systems.

1. Introduction

The rapid advancement of medical technologies in recent decades has caused a significant change in the field of healthcare. Among these innovations, POC technologies have emerged as valuable tools for improving diagnostic efficiency, accessibility, and patient outcomes. Traditionally, medical testing required the collection of specimens and their transport to laboratories for processing, often resulting in significant delays between testing and diagnosis.[1] POC technologies address this limitation by decentralising testing, allowing clinicians, and in many cases patients themselves, to obtain results rapidly in clinical settings, or even at home.[2]

This shift has transformed medical diagnostics by delivering rapid results in a matter of minutes, which is critical for time-sensitive conditions and immediate clinical decision-making.[3,4] Early POC devices included simple tools such as glucometers and urine pregnancy dipsticks. Over time, advances in microfluidics and Lab-on-Chip (LoC) technologies have expanded the capabilities of POC devices to detect a wide array of biomarkers,

pathogens, and physiological parameters. Among available detection strategies, fluorescence-based methods offer distinct advantages that make them well-suited for a wide range of diagnostic applications.[5] One of the key strengths of fluorescence-based detection lies in its high sensitivity and specificity, enabling accurate quantification of diverse analytes in complex biological samples. These methods are based on the exploitation of fluorescent molecules, or fluorophores, which are capable of emitting light upon excitation, allowing for the detection and quantification of target analytes with a high degree of precision. Additionally, fluorescence detection boasts a robust signal-to-noise ratio, rapid response time, and compatibility with miniaturized devices, further enhancing its appeal for POC applications.[6] The improvements in fluorophore design and molecular biology techniques have facilitated the creation of an array of fluorescence-based POC assays, encompassing a diverse range of techniques such as fluorescence resonance energy transfer (FRET), time-resolved fluorescence (TRF), quantum dot-based detection, and single-molecule fluorescence.[7–9] Each of these techniques offers unique advantages; for example, FRET-based assays excel in detecting protein-protein interactions and monitoring enzymatic activities,[10] while quantum dot-based techniques provide exceptional sensitivity and multiplexing capabilities, allowing for the simultaneous detection of multiple targets.[11]

Integrating fluorescence detection with microfluidic and LoC systems has significantly expanded the potential of POC diagnostics.[12] These miniaturized platforms facilitate the analysis of multiple samples while minimizing the volume of reagents and

[a] *Institute of Nanotechnology, National Research Council (CNR-NANOTEC),*
   c/o Campus Ecotekne, via Monteroni, Lecce 73100, Italy.
   E-mail: manuelacedrunmorales@cnr.it, loretta.delmercato@cnr.it

[b] *Department of Biotechnology, School of Life Sciences, Central University of*
   Kashmir, Ganderbal 191201, Jammu and Kashmir, India

[c] *Tecnomed Puglia – Technopole for Precision Medicine (Biotech Lecce Hub),*
   c/o Ecotekne Campus, via Monteroni, Lecce, 73100, Italy

[d] *Department of Experimental Medicine, University of Salento, c/o Campus*
   Ecotekne, via Monteroni, Lecce, 73100, Italy

This journal is © The Royal Society of Chemistry 2026

J. Mater. Chem. C, 2026, **14**, 5607–5628 | **5607**

samples required for testing. Moreover, the development of novel fluorescent probes, such as upconverting nanoparticles (UCNPs) and aggregation-induced emission (AIE) fluorophores, has opened new avenues for enhancing the performance of fluorescence-based POC assays in terms of sensitivity, specificity, and stability.[13,14] Combining fluorescence detection with other emerging technologies, such as smartphone-based imaging and artificial intelligence (AI), has resulted in the development of user-friendly, cost-effective, and highly accurate POC devices. Smartphone-based imaging systems can capture and analyse fluorescence signals, while artificial intelligence algorithms can interpret the data and provide diagnostic results, enabling healthcare professionals to make well-informed decisions regarding patient care.[15,16] These developments also facilitate remote monitoring and telemedicine, broadening access to diagnostic services for underserved and rural populations.

The primary objective of this review is to provide a comprehensive and critical overview of fluorescence-based POC technologies. We discuss the fundamental detection principles, major technological advances, and broad landscape of current applications. Particular emphasis is placed on the integration of fluorescence readout with microfluidic and LoC architectures, which enables rapid, automated, and multiplexed analysis. We then examine the evolution of advanced fluorescent probes, including quantum dots (QDs), UCNPs, and AIE fluorophores, and their impact on assay sensitivity, specificity, and operational robustness. Current limitations and practical constraints, spanning probe stability, matrix interference, standardization, and device miniaturization, are critically assessed. Finally, we outline emerging opportunities and future directions that may drive the next generation of fluorescence-enabled POC platforms, ultimately aiming to enhance diagnostic performance, patient care, and accessibility across clinical, environmental, and resource-limited settings.

2. Fluorescence detection techniques

This section provides an overview of fluorescence-based detection techniques, focusing on the fundamental principles most relevant to sensing strategies, material innovation, and integration into point-of-care (POC) diagnostic platforms.

2.1. Fluorescence spectroscopy

Fluorescence spectroscopy is a powerful analytical technique that exploits the photophysical properties of fluorescent molecules to detect and quantify target analytes in biological samples.[17,18] Upon optical excitation, fluorophores emit light at longer wavelengths, enabling efficient separation of excitation and emission signals and highly sensitive optical readout (Fig. 1).[19,20] The fluorescence response depends on several physicochemical parameters, including temperature, pH, fluorophore concentration, and interactions with the surrounding microenvironment.[21] These dependencies make fluorescence spectroscopy particularly attractive for chemical and biological sensing. Measurements can be performed using steady-state or time-resolved approaches;[20,22] however, steady-state fluorescence is most widely adopted due to its simpler implementation and suitability for miniaturized and portable POC devices.[23–25] Beyond small-molecule fluorophores, fluorescence spectroscopy increasingly relies on nano- and microparticle-based systems, fluorescent proteins, and hybrid constructs. In nanoparticle-based sensors, fluorescent dyes can be incorporated or coupled to the nanostructure, enabling enhanced brightness, improved photostability, and resistance to photobleaching.[26,27] Moreover, the intrinsic optical properties of certain nanomaterials allow spatially resolved detection using microscopy-based readouts, which is advantageous for device-integrated sensing applications.

2.1.1. Fluorescence quenching as a sensing mechanism.
Fluorescence quenching is widely exploited for analyte detection and microenvironmental sensing, as the presence of a quencher reduces fluorophore emission through well-defined photophysical mechanisms (Fig. 2).[28,29] A representative example is the optical sensing of dissolved oxygen using ruthenium-based organometallic complexes, whose fluorescence is dynamically quenched by molecular oxygen.[30–32] These complexes can be incorporated into polymeric or sol–gel matrices, enabling real-time monitoring of oxygen concentration in biological environments.[33,34]
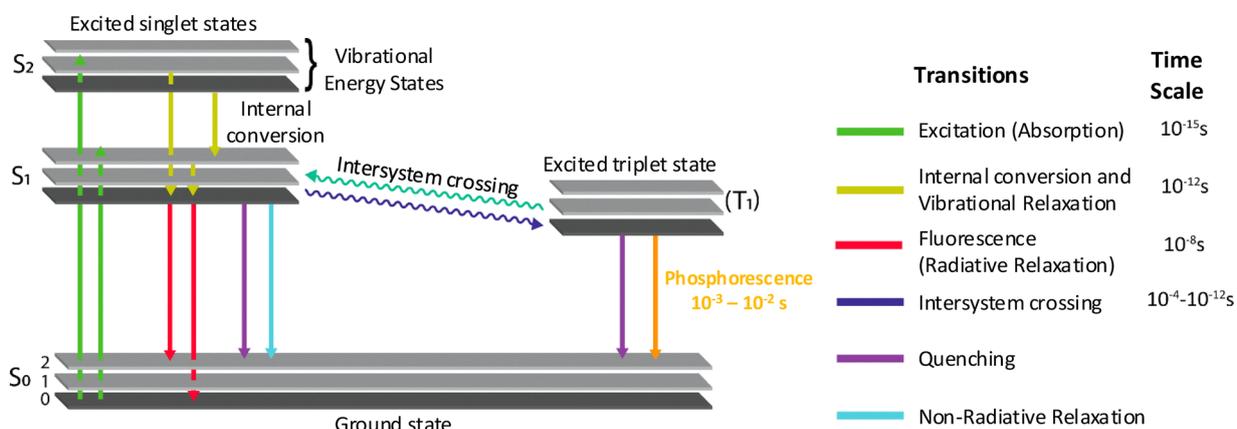

Fig. 1 Jablonski diagram showing excitation, emission and other kinds of transitions of a fluorophore with their associated time scales.

5608 | J. Mater. Chem. C, 2026, 14, 5607–5628

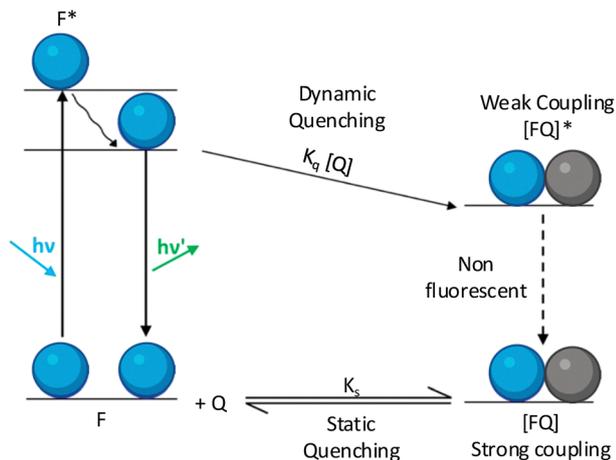This journal is © The Royal Society of Chemistry 2026

Fig. 2 Jablonski diagram showing static and dynamic quenching of a fluorophore. Static quenching as shown is independent of quencher concentration and occurs due to strong coupling between the fluorophore and quencher before excitation. While in dynamic or collisional quenching the excited fluorophore weakly interacts with it and makes it non-fluorescent by non-radiative emission. In dynamic quenching, the degree of quenching is directly proportional to quencher concentration.
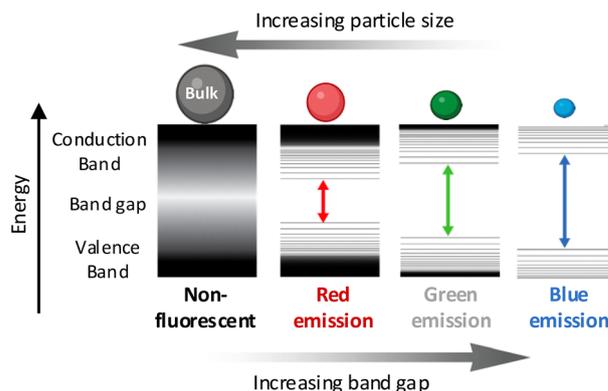

Fig. 3 Size-dependent change in fluorescence emission for semiconducting QDs. The plot illustrates the relationship between QD size and emission wavelength, highlighting the inverse correlation between size and band gap energy. Smaller QDs exhibit a wider band gap, resulting in higher energy emissions (blue light), while larger QDs show a reduced band gap and emit lower energy photons (red light). In bulk materials, the overlapping valence and conduction bands lead to a zero band-gap, and consequently, no emission.

Quenching mechanisms are commonly classified as static or dynamic. Static quenching occurs when the fluorophore and quencher form a non-fluorescent complex before the excitation takes place. In this case, the fluorescence quenching is independent of the fluorophore concentration and is described by the Stern–Volmer equation:[35]

$$\frac{F_0}{F} = 1 + K_{sv}[Q] \tag{1}$$

where F_0 and F are the fluorescence intensities in the absence and presence of the quencher, respectively, [Q] is the quencher concentration, and K_{sv} is the Stern–Volmer constant.

Dynamic quenching occurs when the fluorophore and quencher interact with each other in a collisional encounter. In this case, the fluorescence quenching is dependent on the fluorophore concentration and is described by the modified Stern–Volmer equation:

$$\frac{F_0}{F} = 1 + K_{sv}\frac{[Q]}{[F_0]} \tag{2}$$

where $[F_0]$ is the initial fluorophore concentration.

The distinction between static and dynamic quenching is therefore essential for sensor design, calibration, and interpretation of fluorescence responses in material-integrated sensing platforms.[36]

2.1.2. Fluorescence nanomaterials and quantum dots. Compared to molecular fluorophores, fluorescent NPs display a different behaviour. If the NP fluorescence is due to the presence of small molecular fluorophores, their binding mode and position on the nanoparticle could also significantly affect the overall sensitivity of the resultant nanoparticle sensors towards the analyte that the molecular fluorophore can detect.[37] In the case of semiconducting fluorescent quantum dots (QDs), carbon dots (CDs) and gold nanoclusters (AuNCs), where the photoluminescence is an

intrinsic effect due to the quantum confinement effect or surface defects, the emission can be tailored by optimizing size and composition.[38] A well-established example is the size-dependent emission shift of CdSe QDs, which allows the generation of spectrally distinct probes without chemical modification (Fig. 3).[38] These features make fluorescent nanomaterials particularly attractive for multiplexed sensing and device-integrated optical detection.

2.2. Fluorescence microscopy

Fluorescence microscopy is an imaging technique widely used to visualize the spatial distribution and dynamics of biomolecules in cells and tissues.[39–42] Its application in diagnostics has expanded alongside the development of advanced probes and imaging strategies compatible with live and minimally invasive measurements.[19,43–45] Despite its high sensitivity and specificity, fluorescence microscopy is limited by photobleaching, phototoxicity, and diffraction-limited spatial resolution.[46] Considerable efforts have therefore been directed toward improving image resolution, leading to the development of super-resolution techniques capable of achieving lateral resolutions in the 20–50 nm range.

2.2.1. Principles, probes, and optical configurations. Fluorescence microscopy relies on selective excitation of fluorescent probes and spectral separation of emitted light using dichroic mirrors and optical filters.[19,43,46–49] A wide range of fluorophores, including synthetic dyes and genetically encoded fluorescent proteins, can be introduced into samples through direct labelling, immunofluorescence, or genetic expression.[48–50] Different optical configurations are employed[47] depending on the application, including widefield epifluorescence, confocal, multiphoton, and super-resolution microscopy.[51–53] These platforms support both qualitative imaging and quantitative, imaging-based sensing approaches relevant to diagnostic and device-integrated applications.

This journal is © The Royal Society of Chemistry 2026

J. Mater. Chem. C, 2026, **14**, 5607–5628 | **5609**

2.3. Fluorescence lifetime imaging (FLIM)

Fluorescence lifetime imaging (FLIM) is an advanced optical technique that combines spatial resolution with time-resolved detection to probe molecular interactions and microenvironmental changes beyond intensity-based imaging.[54,55] By measuring fluorescence decay times, FLIM provides concentration-independent contrast that is particularly valuable for sensing applications involving parameters such as pH, viscosity, ion concentration, and protein–protein interactions.[56–58]

In its simplest formulation, the temporal decay of fluorescence intensity following pulsed excitation can be described by a mono-exponential function:

$$I(t) = \alpha e^{-t/\tau}$$

where α is the amplitude of the exponential function and τ is the fluorescence lifetime, which is the time the intensity decreases to α/e.[59]

The fluorescence lifetime reflects the average time a fluorophore remains in the excited state and is highly sensitive to its local molecular environment. As a result, lifetime-based measurements are less affected by variations in fluorophore concentration, excitation intensity, photobleaching, or uneven illumination compared to intensity-based fluorescence imaging.[57]

Fluorescence lifetime can be measured using time-domain or frequency-domain approaches. In time-domain FLIM, the samples are excited with short light pulses and the fluorescence decay is directly recorded, whereas in frequency-domain FLIM, the excitation light is intensity-modulated and lifetime information is extracted from phase shifts in the emitted signal.[55]

FLIM implementations range from widefield to scanning configurations and are compatible with both imaging and non-imaging modalities, including endoscopic and fiber-based systems.[57,60–63] Owing to its robustness and sensitivity to biochemical changes, FLIM has found increasing application in tissue diagnostics and fluorescence-guided procedures, where lifetime contrast enables non-invasive or minimally invasive characterization of biological tissues.[64]

3. Fluorescent probes and labels

Fluorescent probes have been extensively employed not only for sensing, as optical imaging tools, but also for therapy as optical contrast agents or phototherapy agents. Fluorescent molecular probes and labels are made up of two components: a reporter and a recognition unit. The fluorophore, which works as a reporter, emits light upon excitation, while the recognition unit selectively recognizes the given molecular process or targets of interest, translating the recognition event in a well-defined manner into changes of the fluorescence properties of the reporter.[65] Thus, fluorophore reporters are the centerpiece of each fluorescence molecular probe/label that in turn, represents the key components underlying the fluorescence-based POC technologies.

A wide range of probes and labels are available, and the choice depends on the desired application, detection modality,

and sample properties (Fig. 4). Fluorescent compounds can be generally classified into four categories considering their molecular complexity and synthetic methods: small fluorophores made up of molecules of 20–100 atoms,[66] such as organic compounds,[67] and larger fluorophores that include proteins and peptides,[68–70] synthetic oligomers and polymers such as polyfluorenes,[71] and polyphenylene vinylenes,[72] and multi-component systems such as QDs[73,74] and UCNPs.[75,76] These fluorescence probes work by adopting different sensing mechanisms that include FRET, photo-induced electron transfer (PET), intramolecular charge transfer (ICT) and excited state intramolecular proton transfer (ESIPT).[77]

The fluorescence intensity change that occurs when the emission spectrum of a donor overlaps with the adsorption spectrum of an acceptor and the distance between the donor and the acceptor is suitable (<100 Å) is called fluorescence resonance energy transfer and it results in the fluorescence quenching of the donor and fluorescence enhancing of the acceptor.[77,78] Bioluminescence resonance energy transfer (BRET) is a type of FRET where the donor luminophore is represented by a bioluminescent molecule and its electrons are excited by a bioluminescent chemical reaction.[79] The introduction of an analyte can inhibit the energy transfer by changing the dipole, molecular orientation and so on, causing the fluorescence quenching of the acceptor and fluorescence enhancement of the donor.[80,81]

The electron transfer from a receptor (donor) to a fluorophore (acceptor) by intermolecular transfer, called the PET mechanism, leads to fluorescence quenching of the fluorophore. Like FRET, the PET process can be partially or completely inhibited when the receptor binds to the target, causing the restoration of the fluorophore fluorescence.[82]

The electron transfer from a receptor (donor) to a fluorophore (acceptor) by intramolecular transfer, called the ICT mechanism, represents a PET process where the donor and the acceptor are connected by a conjugate linker to form a conjugate system. The electronegativity of the receptor unit changes once the ICT probe interacts with the target and causes a change in the donor–acceptor system. As a consequence, the excitation of the target bound to the ICT probe produces a larger dipole and a change in the excited state due to the change in electron distribution.[83] Hence, ICT probes possess changes in fluorescence intensity and shifts in emission wavelengths as well when they detect analytes.[84]

The four-level photocycle process of the photoinduced tautomerization of a specific enol–ketone is usually referred to as the ESIPT mechanism.[85] The ground state of the ESIPT molecule usually exists in the form of an enol (E) and its photoexcitation leads to intramolecular charge rearrangement. In turn, the intramolecular charge rearrangement causes a simultaneous enhancement of the acidity of the proton donor and the alkalinity of the proton acceptor that rapidly converts the excited enol form (E*) into the excited ketol form (K*).[86] Lastly, the excited ketol K* returns to the original E form after the radiative decay back to the electronic ground state, by reverse proton transfer (RPT).[86]

Recently, POC technologies based on fluorescence imaging have been developed employing the different classes of

5610 | J. Mater. Chem. C, 2026, 14, 5607–5628

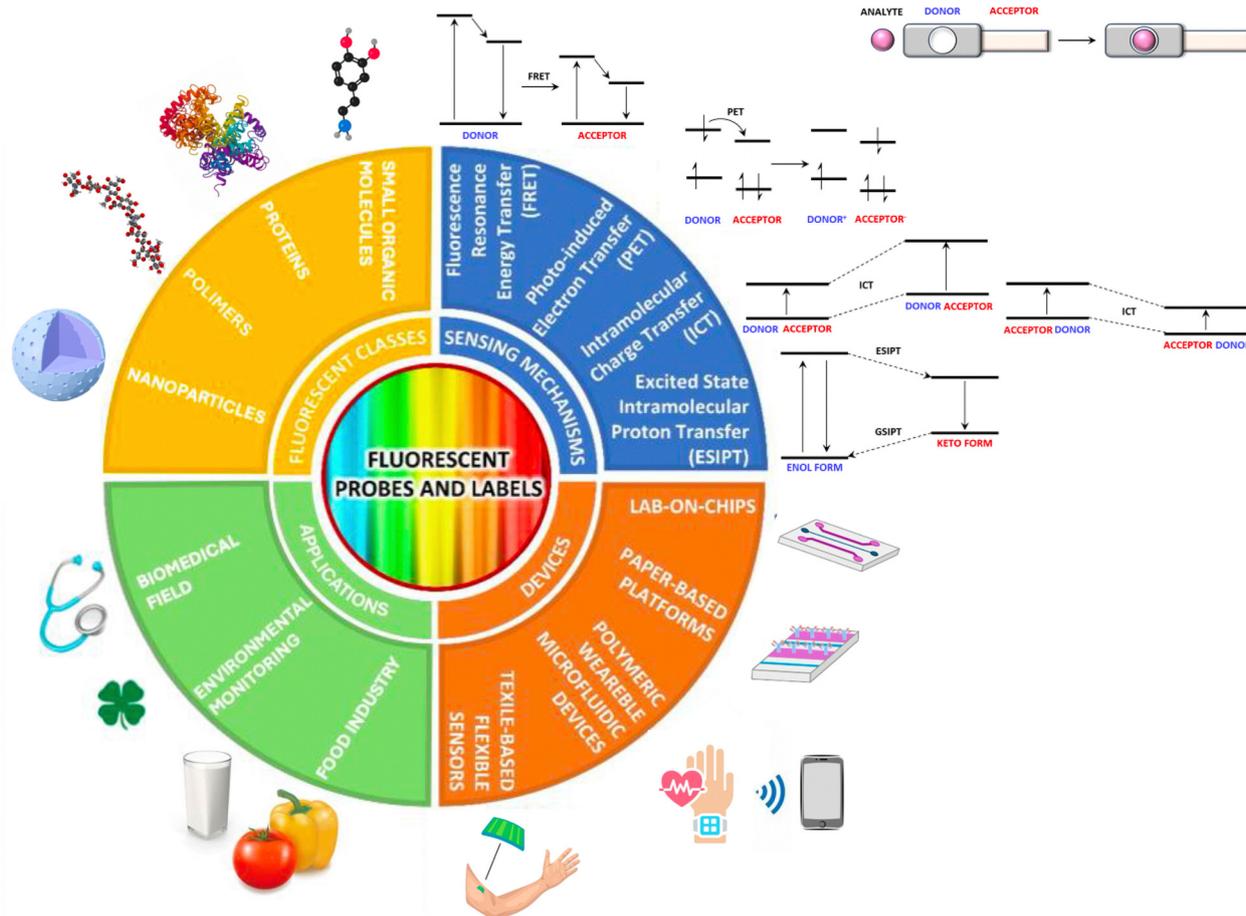This journal is © The Royal Society of Chemistry 2026

Fig. 4 Diagram showing the main features of fluorescent probes and labels for POC testing.

fluorophores and the different mechanisms of fluorescence. Fluorescence in fact appeared as one of the most promising approaches among the different bioimaging and biosensing techniques, such as magnetic resonance imaging (MRI), ultrasound (US), positron emission tomography/computed tomography (PET/CT), single-photon emission computed tomography (SPECT) and computed tomography (CT). Fluorescence allows extreme customization, and selective[69,87] and sensitive[88,89] target analyte detection in complex biological samples, it provides abundant information regarding biomolecules, and it results in a more holistic approach for the imaging of targets in living organisms.[41,90]

3.1. Organic fluorophores

Fluorescent organic fluorophores have been extensively used as raw materials in various biomedical, food industry[91] and textile[92] applications, thanks to their high versatility and their simple operation.[93]

Organic fluorophores include a diverse class of synthetic organic compounds characterized by their ability to absorb light at specific wavelengths and emit fluorescence upon returning to their ground state.[94] Their chemical structure is distinguished by the presence of several combined aromatic groups, or planar or cyclic molecules with different π bonds that generate rigid structures.[94] According to the Woodward–Fieser rules, conjugated systems with fewer than eight double bonds absorb only in the ultraviolet region and appear colorless. Adding more double bonds causes a redshift in absorption, lowering the energy and shifting the color from yellow to red. Fluorogens are dyes that are colorless and non-fluorescent in solution but become fluorescent upon binding to a target, and can also serve as selective fluorescent probes.[95] The Woodward–Fieser rules and other empirically derived guidelines help predict the absorption maximum wavelength in the UV–visible spectrum of a compound, allowing for flexible and customizable design of organic fluorophores.[96] Hence, the photophysical properties of the organic fluorophores can be tuned to obtain specific wavelengths in their absorption and emission spectra,[97] to increase their Stokes shift,[98] to improve fluorophore photostability[99] and to ensure high quantum yields.[100] Additionally, organic fluorophores can be easily designed with functional groups that facilitate their conjugation to scaffolds or target biomolecules, allowing selective labelling, detection and their successful administration into cells.[101–105] Moreover,

This journal is © The Royal Society of Chemistry 2026

J. Mater. Chem. C, 2026, **14**, 5607–5628 | **5611**

organic fluorophores exhibit an inherent high sensitivity and strong specificity with low interference from sample matrices.[69,106] Lastly, organic fluorophores are dyes that can be employed as inks.[107] Thus, they can be printed on absorbent materials to assemble cheap POC devices.

3.1.1. Types and properties. Non-protein organic fluorophores belong to several major chemical families, each with distinct photophysical and chemical properties that make them valuable for a wide range of applications. Acridine derivatives (*e.g.*, acridine orange, acridine yellow, and riboflavin) are characterized by long fluorescence lifetimes and are widely used for labeling biological molecules.[108,109] Anthracene derivatives (*e.g.*, anthraquinones) exhibit excellent cell membrane permeability and good photobleaching resistance in living cells.[110,111] Arylmethine derivatives (*e.g.*, auramine, crystal violet, and malachite green) are known for their high quantum yields, while coumarin derivatives provide large Stokes shifts, making them ideal for imaging applications.[112,113] Cyanine derivatives feature narrow absorption bands and exceptionally high extinction coefficients, contributing to their sensitivity. Dipyrromethene derivatives (*e.g.*, BODIPY) are highly sensitive and selective toward metal ions.[114] Naphthalene derivatives display high quantum yields, excellent photostability, and strong ion sensing capabilities for both anions and cations.[114–116] Oxadiazole derivatives (*e.g.*, pyridyloxazole, nitrobenzoxadiazole, and benzoxadiazole) are valued for their high thermal stability and fluorescence efficiency.[117] Oxazine derivatives (*e.g.*, cresyl violet, brilliant cresyl blue, Nile red, Nile blue, and Oxazine 170) are notable for their chemical stability and lipophilic nature.[118] Pyrene derivatives (*e.g.*, cascade blue and HPTS) are distinguished by their strong fluorescence emission in live cells, low cytotoxicity, high quantum yield, and excellent cell permeability.[119,120] Squaraine derivatives are efficient two-photon absorbers, characterized by intense and narrow absorption and emission in the visible and near-infrared regions, combined with high photostability and low biotoxicity.[121] Xanthene derivatives (*e.g.*, fluorescein, rhodamine, Oregon green, eosin, and Texas red) possess excellent photochemical properties in aqueous environments, high fluorescence quantum yields, and suitable absorption/emission maxima for deep tissue imaging and both *in vitro* and *in vivo* dynamic imaging.[122–125] Lastly, tetrapyrrole derivatives (*e.g.*, porphin, phthalocyanine, and bilirubin) exhibit high excitation coefficients, strong emission efficiency, and exceptional photostability and quantum yields across various solvents, allowing for versatile use in multiple detection scenarios without solvent limitations.[126]

3.1.2. Applications. Organic fluorophores are successfully integrated in POC technological (POCT) devices for immunoassays, nucleic acid detection, cell imaging, and biosensing serving as direct labels, FRET donors or acceptors, or components of fluorescence-based probes, such as molecular beacons or aptamer-based sensors, enabling the sensitive and specific detection of target analytes. We report some recent POCT devices made up of LoCs,[89] mobile phones,[127] or paper-based platforms that integrate fluorescent dyes for the portable, field deployable, accurate, rapid and affordable detection of analytes of interest.[128]

Cai *et al.* developed a reliable lateral flow immunoassay (LFIA) by a facile one-step synthesis of red fluorescent microspheres containing Nile Red, enhancing stability and reducing background noise (Fig. 5A).[129] By combining this with immunochromatography, they established a new POC testing platform for the rapid and early detection of cardiac troponin I (cTnI), a cardiac-specific biomarker for acute myocardial infarction (AMI).

Sekine *et al.* developed a wearable PDMS microfluidic device with fluorescent probes for real-time sweat analysis (Fig. 5B).[130] Paired with a smartphone, it detects chloride, sodium, and zinc, demonstrating portable, continuous biomarker monitoring.

Ghassemi *et al.* explored contrast-enhanced near-infrared (NIR) fluorescence imaging using a mobile phone-based POC testing platform, employing indocyanine green (ICG) to visualize tissue perfusion and vasculature. Imaging on tissue phantoms and an *ex vivo* model confirmed the feasibility of mobile NIR imaging and highlighted performance variations based on wavelength, pixel color, and image processing.[131]

Lei He *et al.* developed a compact, integrated device for rapid and accurate screening of bovine mastitis *via* somatic cell counting (SCC). The system combines a custom cell-counting chamber pre-loaded with acridine orange dye and a miniature fluorescent microscope, providing a simple and practical POC diagnostic solution.[132]

Pharmacogenetic (PGx) testing and theranostics are essential components of personalized medicine, leveraging genetic variations such as single nucleotide polymorphisms (SNPs) to explain individual differences in drug response.[133] For instance, the Spartan RX CYP2C19 system enables POC genotyping to guide antiplatelet therapy. Buccal swabs are collected in individual kits containing swabs and reagent tubes specific for the CYP2C19 *2, *3, and *17 alleles. The platform automates DNA extraction, PCR amplification, allele detection, and genotyping, using fluorescent-labeled probes and optical detection channels to identify each variant, with a sensitivity of 0.1 ng μL^{-1}.[134]

Continuous monitoring of body fluids plays a vital role in modern healthcare by enabling early detection of health changes, improving treatment outcomes, and reducing the risk of complications. Tears, for example, known to closely reflect blood biomarker levels, are a valuable, non-invasive source for assessing eye health.[135]

Yetisen *et al.* developed a fluorescent wearable scleral lens sensor for POC diagnosis of ocular diseases through quantitative tear analysis. The device measures pH and five key ions (Na^+, K^+, Ca^{2+}, Mg^{2+}, and Zn^{2+}) at physiological levels using specialized fluorescent probes embedded in an engraved scleral lens. The system includes a portable readout device with LEDs and optical filters, coupled with smartphone-based data processing and user interface. This integrated approach enables assessment of dry eye severity stages and differentiation of disease subtypes.[136,137]

Finally, the AFIAS IFX is an automated fluorescence lateral flow immunoassay for rapid POC monitoring of infliximab levels in patients with intestinal bowel disease (IBD). Unlike traditional ELISA testing that takes days, this system delivers
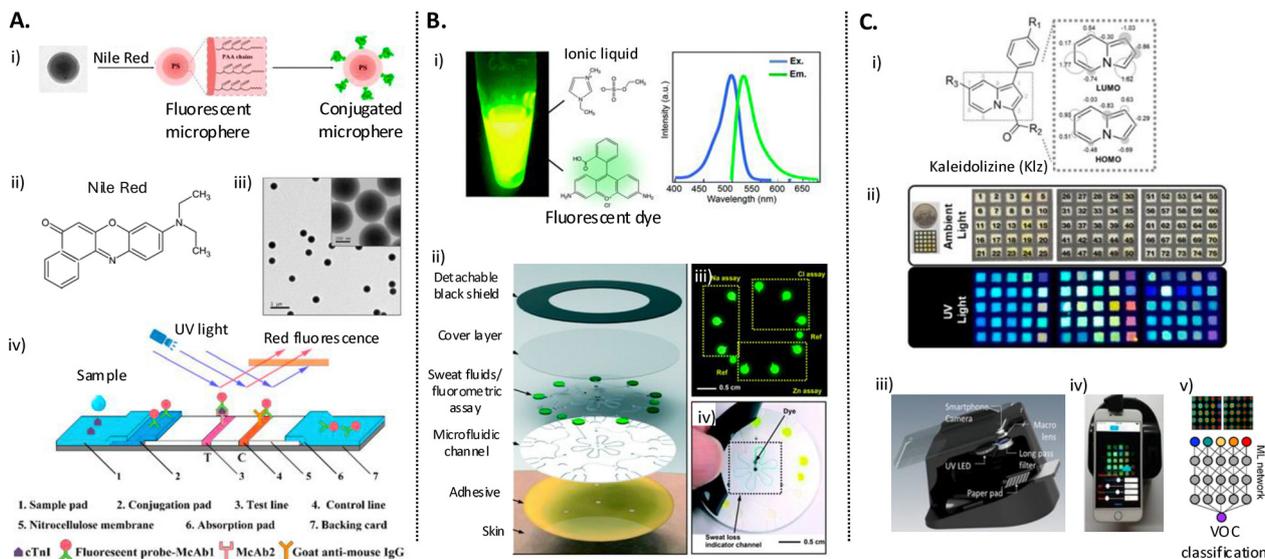
5612 | *J. Mater. Chem. C*, 2026, **14**, 5607–5628

This journal is © The Royal Society of Chemistry 2026

Fig. 5 (A). PS microspheres functionalized with carboxyl groups *via* copolymerization of styrene and acrylic acid, labeled with Nile Red, and bioconjugated with anti-cTnI antibodies. (i) Schematic of the preparation. (ii) Structure of Nile Red. (iii) TEM images showing uniform morphology. (iv) Sandwich-type LFIA for cTnI detection: the sample migrates, binds fluorescent probe-McAb1, and is captured by immobilized McAb2 on the test line; the control line captures excess probes; fluorescence quantified under UV. Reproduced with permission[129] copyright 2018 MDPI. (B) Skin-interfaced microfluidic device for sweat analysis of Cl⁻, Na⁺, and Zn²⁺. (i) Stable fluorescent reference dye in ionic liquid with excitation/emission spectra. (ii) Schematic of the multilayer microfluidic platform for sweat collection and *in situ* assays. (iii) Fluorescence images of the embedded chemical probes. (iv) Peeling the detachable black shield reveals sweat indicator channels. Reproduced with permission[130] copyright 2018 Royal Society of Chemistry. C. Fluorescent compound array for portable chemical classification. (i) Kaleidolizine (Klz) structure and HOMO/LUMO orbital illustration. (ii) Array of 75 Klz derivatives on wax-printed cellulose under ambient and UV light; inset shows size comparison. (iii) 3D cradle device for smartphone-based detection. (iv) Photograph of the device in operation. (v) Automated fluorescence pattern analysis using machine learning for VOC classification. Reproduced with permission[139] copyright 2021 Elsevier.

quantitative results in 20 minutes using an all-in-one cartridge (comprising sample dilution buffer, antibody conjugators, and a strip). This enables clinicians to check infliximab levels immediately before infusion and make real-time dosage decisions, improving therapeutic drug monitoring and patient outcomes.[137]

Beyond clinical diagnostics, fluorescence-based POCT devices have recently expanded into the environmental and food safety sectors. In the field of water quality monitoring, Leonard *et al.* introduced a smartphone-enabled POC platform for the rapid quantification of microplastics in water using Nile Red fluorescence staining. A 3D-printed attachment and custom app enable semi-automated analysis of particles as small as 20 μm within 10 minutes. The portable, cost-effective system showed strong agreement with lab microscopy and works on synthetic and environmental samples, making it suitable for field monitoring and community-led research.[138]

Fluorescence-based sensing platforms are increasingly being adapted for POC chemical detection in air, proving their high sensitivity and rapid response. Kim *et al.* developed a fluorescent sensor array combined with machine learning to enable portable, low-cost, and multiplex detection of VOCs (Fig. 5C).[139] Environment-sensitive dyes printed on a substrate generate unique fluorescence "fingerprints" upon analyte exposure, captured by a smartphone or portable imager. Convolutional neural networks (CNNs) analyze the patterns, accurately identifying VOCs such as toluene, acetone, and ethanol within

≤5 minutes, demonstrating a smart, field-ready platform for air quality monitoring.

Zhang *et al.* developed a wearable fluorescent POC sensor based on a newly synthesized hydroxynaphthalene benzophenone Schiff base (HNPBS).[140] The fluorophore exhibits strong and selective emission responses to airborne VOCs such as acetone, acetonitrile, ethanol, and formaldehyde. Integrated into a flexible polymeric film, it functions as a low-cost, portable platform for real-time on-body detection. The sensor operates *via* fluorescence shifts from blue to green upon VOC exposure, arising from specific interactions between analytes and amine groups in the matrix. It provides distinct optical signatures for various VOCs, fast response (<30 s), good reversibility, and high selectivity under ambient conditions, making it highly suitable for personal exposure and indoor air quality monitoring within decentralized POC diagnostics.

Fluorescence based POC technologies have shown exceptional effectiveness for food safety monitoring, enabling the sensitive detection of pathogens, toxins, heavy metals, and antibiotic residues even at trace levels.[15,141,142] Cheng *et al.* developed a dual-target lateral flow immunoassay (LFIA) enhanced with peroxidase-mimicking Pd@Pt core–shell nanozymes for the simultaneous detection of *Salmonella Enteritidis* and *Escherichia coli* O157:H7 in food samples.[143] Acting as catalytic antibody labels, the nanozymes replaced conventional enzymes such as horseradish peroxidase and generated a strong colorimetric signal upon reaction with TMB/H₂O₂. This

This journal is © The Royal Society of Chemistry 2026

J. Mater. Chem. C, 2026, **14**, 5607–5628 | **5613**

amplification strategy enabled ultrasensitive detection limits of 20 CFU mL^{-1} for Salmonella and 34 CFU mL^{-1} for *E. coli*. The portable assay was fully compatible with a 3D-printed smartphone-based reader, demonstrating high recovery and accuracy in real food matrices.

Further expanding the application scope to toxic metal detection, Shan *et al.* developed a portable fluorescence biosensor for selective and sensitive detection of Hg^{2+} ions in food, based on thymine–Hg^{2+}–thymine (T–Hg^{2+}–T) coordination chemistry.[144] The sensor uses a fluorescent DNA probe that changes intensity upon binding mercury, ensuring high selectivity over other metals. Integrated with a miniaturized smartphone-based fluorescence microscope, the system excites samples with LED light and captures emission *via* the phone camera for real-time quantification. With a low detection limit of 0.33 nM, the compact and user-friendly platform enables on-site mercury monitoring in food without lab equipment, ideal for resource-limited settings.

3.2. Fluorescent proteins

Fluorescent proteins (FPs) have revolutionized the field of molecular and cellular biology by providing researchers with a unique and powerful colour palette to visualize and monitor a wide range of biological processes with unprecedented precision. The first FP, green fluorescent protein or GFP, was discovered in 1962 by the Japanese biochemist Osamu Shimomura, from the bioluminescent jellyfish Aequorea Victoria.[145] Thanks to the discovery of such a powerful tool, he was awarded with the Nobel prize in chemistry in 2008, along with Roger Y. Tsien and Martin Chalfie. The wild type GFP is a 238 amino acid long protein, with a molecular weight of 27 kDa. It displays a β-barrel tertiary structure composed of 11 β-strands and 2 small α-alpha helices, one on the top of the barrel and one on the bottom. The chromophore portion of the protein is located between these α-helix segments. The chromophore of the GFPs derives from the subsequent cyclization and oxidation of a tripeptide (Ser65, Tyr66 and Gly67) that leads to the formation of an imidazoline moiety with conjugated double bonds. A similar structure is also present in the red fluorescent protein or DsRed, first isolated from the red coral of the *Discosoma genus*.[145]

3.2.1. Types and properties. All the fluorescent proteins available are derived from the mutagenesis of GFP and DsRed. The engineering of these two proteins gave researchers a plethora of fluorescent proteins that cover the full spectrum of visible light. However, the excitation wavelength and emission wavelength are not the only parameters that have been optimized for FPs. There are a multitude of variants with improved quantum yield, improved resistance to photobleaching, shorter maturation times (the maturation time of DsRed is 24 hours), low cytotoxicity and better expression.[146,147] For the expression of chimeric proteins, there are also optimized variants to prevent the oligomerization of FPs. Engineered FPs are creatively named after the colour of fruits and their quaternary structure, *e.g.* mCherry is a monomer with cherry colour, while tdTomato is a tandem dimer with tomato

colour.[148] Other parameters that can influence the performance of FPs are pH (some FPs are pH sensitive), oxygen (oxygen is a substrate for the chromophore formation), ion concentration (yellow fluorescent proteins (YFPs) are sensitive to Cl$^-$ concentration), maturation temperature (FPs have different performance on different temperature) and optimization of heterologous expression. This latter parameter can be solved by using species-specific codon-optimized FPs.

3.2.2. Applications. Over the years, scientists have harnessed the power of FPs to investigate cellular and molecular phenomena in living organisms. By genetically engineering cells to express FPs fused to specific target proteins or organelles, researchers can visualize the dynamics of cellular structures with unprecedented clarity. FPs can also be used as genetically encoded biosensors, which are designed to detect and respond to specific target molecules or events within a cell or biological system. A genetically encoded biosensor (GEB) is composed of two parts: a molecular recognition element (MRE) and an optical reporter.[149] The MRE can derive from the sequence of a membrane receptor, a protein binding domain or an antibody, while the optical reporter is an FP that undergoes a conformational rearrangement that can quench or enhance its fluorescence emission. FPs have been successfully employed for Ca^{2+} sensing by imaging in neural networks (Fig. 6A).[150,151] GEBs are not the only types of biosensors that were obtained with FPs; different assays were developed to detect and quantify proteins and specific antibodies in human blood serum (Fig. 6B).[152,153] Among fluorescent protein platforms, flavin-binding fluorescent proteins (FbFPs) based on engineered light, oxygen, and voltage (LOV) domains represent a promising alternative to traditional GFP-like proteins. Recently, a directed molecular evolution approach was applied to develop two miniaturized FbFPs, termed miniGFP1 and miniGFP2, with excitation/emission maxima at 450/499 nm and a compact molecular size of approximately 13 kDa (Fig. 6C).[154] Systematic benchmarking in *E. coli* and mammalian cells revealed that miniGFPs exhibit enhanced photochemical stability and superior performance compared to previously available FbFPs, enabling long-term live-cell imaging under both aerobic and anaerobic conditions. Importantly, miniGFPs demonstrated nanomolar sensitivity to Cu(II) ions ($K_d \approx$ 67–68 nM) and fluorescence quenching by Cu(I), indicating their potential use as optical indicators for copper redox states. Additionally, their selective binding to flavin mononucleotide suggests applications as specific fluorescent flavin sensors. Altogether, these miniGFPs represent a multisensing and oxygen-independent fluorescent platform for *in vitro* and in-cell biosensing applications.

3.3. Fluorescent nanomaterials

Besides QDs or UCNPs, fluorescence POC technologies can be based on other nanomaterials, such as metal nanoparticles (MNPs),[155] metal–organic frameworks (MOFs),[156] silica nanoparticles (SiNPs), or carbon-based nanomaterials (Fig. 7).[157] These systems combine structural tunability, high surface-to-volume ratios, and unique optical behaviours, properties that make them adaptable for sensing and diagnostic applications.
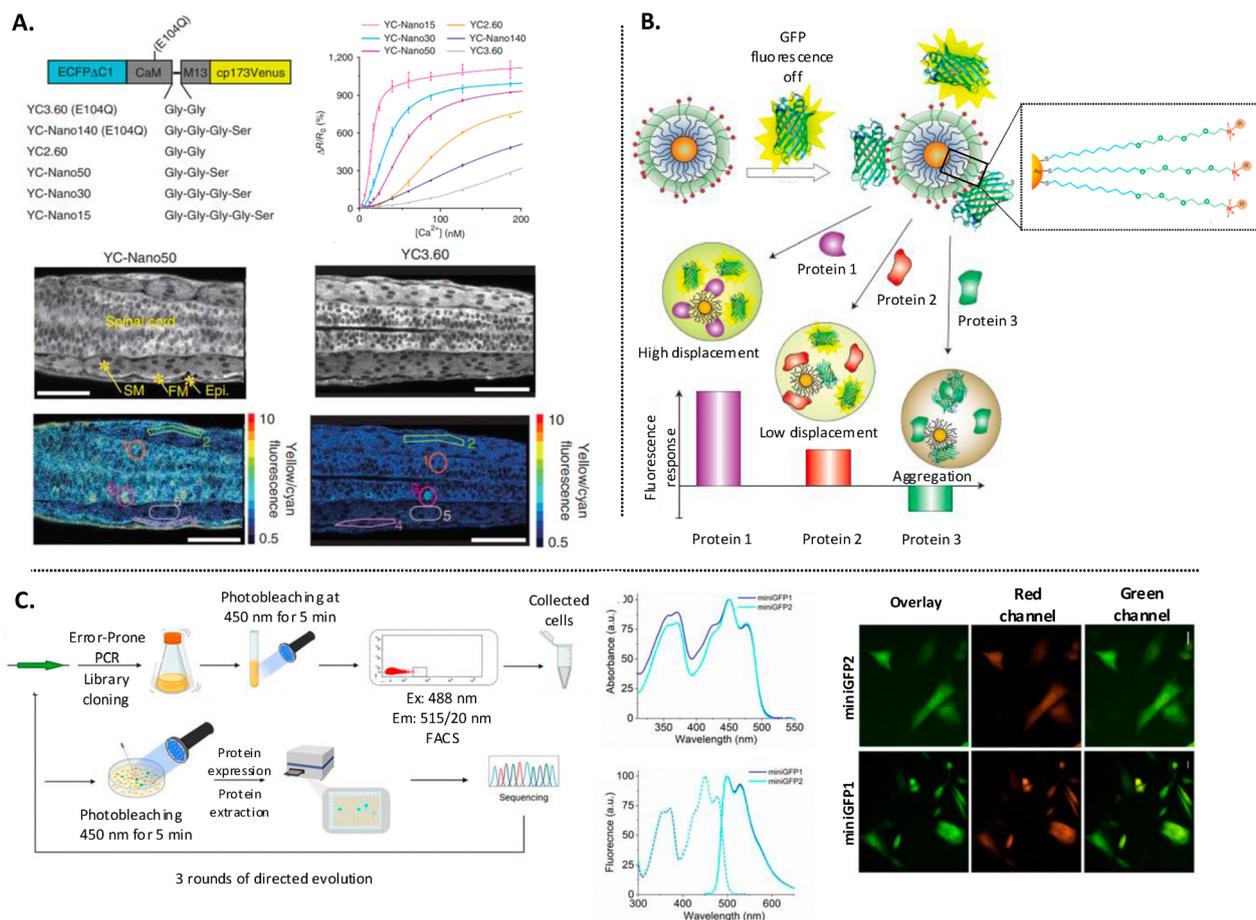
5614 | *J. Mater. Chem. C*, 2026, **14**, 5607–5628

This journal is © The Royal Society of Chemistry 2026

Fig. 6 (A). YC-Nano Ca^{2+} indicators. Top-left: peptide linker design connecting CaM and M13; YC3.60 and Nano140 contain CaM(E104Q), M13 binds Ca^{2+}-loaded CaM, ECFPΔC11 is truncated CFP, cp173Venus is circularly permuted Venus. Top-right: Ca^{2+} titration curves ($\Delta R/R_0$ vs. $[Ca^{2+}]$; $n = 3$). Bottom: Confocal images of living zebrafish embryos injected with YC-Nano50 (left) or YC3.60 (right) showing spontaneous motor activity (yellow fluorescence), with corresponding Y/C ratio images; segmented musculature (SM, FM) lies between the spinal cord and epidermis. Scale bars, 50 μm. Reproduced with permission[151] copyright 2010 Nature Publishing Group. (B) Nanoparticle (NP) sensor mechanisms. Schematic of protein interactions with quenched GFP–NP complexes *versus* protein aggregation, yielding fluorescence enhancement or additional quenching. NP1: cationic; NP2/NP4: hydrophobic; NP3: hydrogen bonding; NP5: aromatic π–π recognition. Reproduced with permission[153] copyright 2009 Nature Publishing Group. (C) Engineering small GFPs. Left: Directed evolution strategy of flavin-binding miniGFPs in *E. coli* using FACS. Center: absorbance, excitation/emission spectra, and biochemical profiling relative to phiLOV3, CreiLOV, and BR1. Right: Representative fluorescence images of CHO cells expressing miniGFPs in the green/red channels. Scale bar, 20 μm. Reproduced with permission[154] copyright 2022 Frontiers Media S.A.
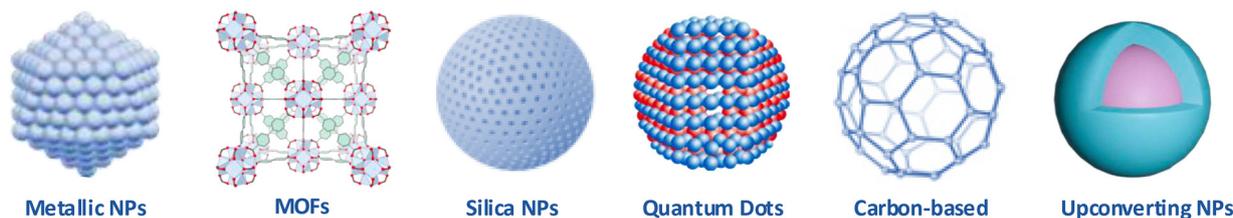

Fig. 7 Types of nanoparticles employed in fluorescence-based POC technologies.

Unlike molecular dyes or proteins, particle-based probes offer enhanced photostability, opportunities for surface functionalization, and strong signal amplification mechanisms that improve sensitivity in POC biosensors.[158] Their fluorescence properties can originate from intrinsic photoluminescence, dye encapsulation, plasmonic effects, or hybrid organic–inorganic interactions, providing a wide range of detection strategies. In the next section, we will show an overview regarding these nanomaterials.

3.3.1. Types and properties

3.3.1.1. Metal nanoparticles (MNPs). MNPs, particularly gold (AuNPs) and silver nanoparticles (AgNPs), are among the most

This journal is © The Royal Society of Chemistry 2026

J. Mater. Chem. C, 2026, **14**, 5607–5628 | **5615**

widely explored fluorescent platforms for POC applications due to their unique plasmonic properties.[159] These particles exhibit strong localized surface plasmon resonance (LSPR), which generates intense electromagnetic fields in their immediate vicinity. When placed near fluorescent molecules, these fields can significantly enhance excitation and emission rates, a phenomenon known as metal-enhanced fluorescence (MEF). The enhancement depends critically on particle parameters such as size, shape, composition, and architecture, including core–shell structures, alloys, or surface-decorated designs, allowing precise tuning of optical responses.

The interaction between metallic NPs and fluorophores creates hybrid systems, where the emission of photons from the fluorophore can excite plasmonic oscillations in the metal, producing new radiative decay pathways.[160] In this configuration, both excitation and radiative decay rates increase, leading to stronger emission signals. As a result, fluorescence detection achieves higher sensitivity, allowing the observation of weakly emitting species that would remain undetectable in other cases. Moreover, photostability is improved because the reduced fluorescence lifetime decreases the time of probes in the excited state. In addition, MNPs can also act as scattering centers or energy donors, enabling sensitive detection even at the single-molecule level.[161]

In POC diagnostics, MNPs have been widely incorporated into lateral flow assays, microfluidic devices, and chip-based sensors.[162] Their strong plasmonic properties not only provide rapid and ultrasensitive detection of biomolecules such as proteins, nucleic acids, and pathogens, but also enable multiplexed readouts, improved signal-to-noise ratios, and lower detection limits compared to conventional fluorescence-based assays. Furthermore, their tunable optical responses, ease of surface functionalization, and compatibility with portable detection systems make them highly attractive for the development of cost-effective, miniaturized, and field-deployable diagnostic platforms.[163]

Beyond biosensing, MNPs are also applied in forensics, food safety, drug testing, and environmental monitoring, highlighting their versatility as fluorescent nanoprobes. The combination of tunable optical properties, biocompatibility, and facile surface functionalization makes MNPs indispensable tools in the development of next-generation POC technologies.[164]

3.3.1.2. Metal–organic frameworks (MOFs).
MOFs are a distinctive class of crystalline hybrid nanomaterials formed by the coordination of metal ions or clusters with multidentate organic ligands, giving rise to highly ordered, porous architectures.[165,166] Their modularity allows enormous structural and chemical diversity, enabling precise control over pore size, surface area, and chemical functionality. Importantly, many MOFs exhibit intrinsic photoluminescence due to their organic linkers or metal centers, while others can be engineered as hybrid fluorescent platforms by incorporating dyes, QDs or rare-earth elements into their frameworks.[156] This tunability provides MOFs with a high degree of flexibility for optical sensing and POC applications.

The luminescence mechanisms in MOFs may arise from several processes, including ligand-centered emission, metal–

ligand charge transfer, or guest–host interactions within their porous cavities.[167] These properties can be further modulated by tailoring the organic linker chemistry or by selecting specific metals (e.g., Zn, Zr, and lanthanides) to introduce new electronic transitions. Moreover, the porous structure of MOFs not only improves their fluorescence stability by shielding encapsulated fluorophores from quenching, but also provides selective recognition sites for analytes, creating turn-on, turn-off, or ratiometric fluorescent responses.[165]

In the POC landscape, fluorescent MOFs are gaining attention for biomarker detection, environmental monitoring, and multiplexed sensing, as they can combine signal generation with selective analyte capture.[168] Thanks to their porous structure and tunable optical properties, MOFs can combine signal generation with selective analyte capture. Their large surface area allows efficient loading of biomolecules or fluorescent reporters, while their modular composition makes it possible to adjust emission characteristics and recognition sites. These features contribute to improving sensitivity and specificity in complex samples. In addition, the ability to design MOFs with tailored luminescence responses supports their integration into portable and multiplexed POC devices.[169]

3.3.1.3. Silica nanoparticles (SiNPs).
SiNPs represent one of the most established classes of nanomaterials in fluorescence-based sensing due to their particular features, such as their tunable structures, optical transparency, high biocompatibility and ease of surface functionalization.[170,171] Their popularity arises from their role as carriers that can encapsulate fluorescent dyes or QDs within a protective silica matrix, shielding them from photobleaching, solvent effects, and environmental degradation. This strategy not only enhances the photostability and brightness of the fluorophores but also ensures reproducible emission over long-term measurements, which is crucial for POC applications.[172]

What makes SiNPs fascinating from a nanotechnology point of view is their well-defined and tunable structures (i.e. size, morphology, and porosity) and surface chemistry. By introducing new functional groups via well-established siloxane chemistry, the silica surface can be modified to impart new properties to the particles, such as diagnostic and therapeutic capabilities. SiNPs are effectively "transparent" in the sense that they do not absorb light in the NIR, visible, and ultraviolet regions or interfere with magnetic fields. In addition, SiNPs are economic, easy to prepare, relatively chemically inert, biocompatible, and water dispersible.

Fluorescent SiNPs are generally prepared either by dye-doping during synthesis (e.g., via sol–gel or Stöber methods) or by surface conjugation with organic fluorophores or biomolecules. Both approaches allow fine control over size, porosity, and surface charge, making SiNPs adaptable to a wide variety of detection strategies.[173–175] In addition, their surfaces can be easily modified with silane chemistry, polymers, or biomolecular ligands, enabling specific recognition of nucleic acids, proteins, or pathogens. The use of mesoporous SiNPs (MSNs) further expands their potential, as the porous architecture offers high

5616 | J. Mater. Chem. C, 2026, **14**, 5607–5628

This journal is © The Royal Society of Chemistry 2026

loading capacity for dyes, drugs, or enzymes, while also facilitating efficient diffusion of analytes.

In the POC setting, dye-doped SiNPs have been successfully integrated into lateral flow assays,[176] microfluidic devices,[177] and multiplex immunoassays,[178] where they serve as bright, stable, and cost-effective probes.[179] Their strong fluorescence signals improve sensitivity compared to conventional organic dyes, while their robustness ensures compatibility with portable devices and long-term storage. Moreover, SiNP-based probes are being explored for ratiometric sensing,[180–182] real-time monitoring, and combined therapeutic–diagnostic (theranostic) applications, underscoring their versatility.[183]

3.3.1.4. Quantum dots (QDs). Quantum dots are nanosized semiconductor particles with exceptional optical and electronic properties that arise from quantum confinement effects, which occur when charge carriers are confined within dimensions smaller than the exciton Bohr radius.[184,185] This confinement produces discrete energy levels, allowing precise control of the absorption and emission spectra based on particle size and composition.

One of the most distinctive features of QDs is their size-tunable fluorescence: smaller QDs emit light at shorter wavelengths (blue region), while larger ones emit at longer wavelengths (red region).[185,186] This tunability, combined with their broad absorption bands and narrow, symmetric emission peaks, enables simultaneous excitation of multiple QDs and highly multiplexed detection in fluorescence-based assays. Additionally, QDs exhibit exceptional photostability, high quantum yield, and resistance to photobleaching, outperforming conventional organic dyes and many other fluorophores.

From a materials standpoint, QDs are generally composed of group II–VI semiconductors (*e.g.*, ZnS, CdS, CdSe, CdTe, and ZnO), group III–V compounds (*e.g.*, InP, GaN, and GaAs), or group IV–VI materials (*e.g.*, Si, Ge, and carbon-based QDs).[186,187] The selection of the semiconductor core determines the emission range, while core–shell architectures are often employed to improve quantum yield, chemical stability, and biocompatibility. In these systems, a semiconductor core is encapsulated by another material with a wider band gap (*e.g.*, CdSe/ZnS or InP/ZnS), which passivates surface defects and minimizes nonradiative recombination.

QDs can be synthesized using top-down methods (such as lithography or etching) or bottom-up techniques, including wet-chemical and vapor-phase routes.[188] Surface modification plays a crucial role in determining colloidal stability, solubility, and biological compatibility. Functionalization with polymers, ligands, peptides, or antibodies allows target-specific recognition and facilitates integration into biosensors or microfluidic systems.

In the context of POC diagnostics, QDs serve as robust and bright fluorescent probes,[189] enabling sensitive detection of nucleic acids, proteins, and pathogens.[184] Their narrow emission bandwidths make them ideal for multiplexed assays, while their photostability ensures reliable signal retention over prolonged analyses. Despite these advantages, challenges such as

potential cytotoxicity (particularly for cadmium-based QDs) and fluorescence intermittence (*blinking*) remain areas of ongoing research.

3.3.1.5. Carbon-based particles. Carbon-based NPs, including CDs, graphene QDs (GQDs), and nanodiamonds, have emerged as a versatile class of fluorescent nanomaterials, attracting attention due to their low toxicity, biocompatibility, aqueous solubility, and sustainable synthesis.[190] Unlike traditional semiconductor QDs, which often contain toxic heavy metals, carbon-based nanostructures offer an environmentally friendly alternative without compromising photoluminescent performance.[191] Their fluorescence typically arises from a combination of quantum confinement effects, surface defect states, and functional groups, which can be modulated by heteroatom doping (*e.g.*, N, S, and P) or by chemical surface modifications.[192]

Among them, CDs are the most studied, typically synthesized through simple and scalable methods such as hydrothermal carbonization, microwave-assisted reactions, or pyrolysis of organic precursors, including biomass.[193] CDs exhibit excitation-dependent emission, high photostability, and tunable fluorescence, making them promising candidates for multiplexed detection strategies.[194] Similarly, GQDs combine the optical properties of QDs with the electronic and mechanical advantages of graphene, while nanodiamonds offer stable fluorescence from nitrogen-vacancy centers, suitable for bioimaging and sensing under demanding conditions.[195]

In the POC diagnostic landscape, carbon-based NPs have been integrated into fluorescence biosensors, lateral flow assays, and microfluidic devices for the detection of nucleic acids, proteins, and microbial pathogens.[196,197] Their strong quenching ability has also been exploited in FRET–based assays, where target binding induces measurable changes in emission. Furthermore, their intrinsic biocompatibility allows safe use in intracellular imaging, drug delivery tracking, and metabolite monitoring, expanding their role beyond conventional biosensing. Taken together, carbon-based nanomaterials combine eco-friendliness, low cost, and tunable photophysics, positioning them as sustainable alternatives for next-generation POC fluorescence technologies.

3.3.1.6. Upconverting nanoparticles (UCNPs). UCNPs or upconverting nanoparticles have emerged as a promising class of nanomaterials, gaining significant interest in various scientific disciplines due to their unique ability to convert low-energy excitation into high-energy emission.[198,199] UCNPs exhibit anti-Stokes luminescence, wherein two or more low-energy photons are sequentially absorbed, leading to the emission of a single higher-energy photon. This property makes them particularly attractive for fluorescence-based applications, as they exhibit minimal background autofluorescence, high photostability and deeper penetration in living tissues, which could make them ideal for real-time *in vivo* imaging.

UCNPs are typically composed of inorganic NPs based on $NaYF_4$, doped with lanthanide cations in a core–shell manner or in a host–matrix system.[198] Lanthanide cations (Ln^{3+}) are essential for the upconversion phenomenon and the most

This journal is © The Royal Society of Chemistry 2026

J. Mater. Chem. C, 2026, **14**, 5607–5628 | **5617**

widely used are Ytterbium (Yb^{3+}), Erbium (Er^{3+}) and Thulium (Tm^{3+}).[200] The photophysical properties of UCNPs are strictly connected to their size, shape and surface functionalization; these properties are related to the synthetic methods.

The synthesis of lanthanide-doped UCNPs can be performed with different strategies; usually, thermal decomposition and hydro(solvo)thermal synthesis allow monodisperse and regular nanoparticles to be obtained.[201] However, they require high temperature and pressure, and the use of highly hydrophobic solvents (*e.g.*, oleate), producing UCNPs with hydrophobic surfaces that can be dispersed only in nonpolar solvents. Microwave-assisted synthesis offers milder reaction conditions and can be performed in the liquid or solid phase. The easiest way to synthesize UCNPs is coprecipitation, using EDTA as a capping agent, although this method typically yields particles with a broad size distribution, irregular morphology, and low quantum yield.

Despite being considered highly promising for bioimaging, with several advantages compared to QDs, UCNP technology still requires substantial improvement. Their quantum yield remains significantly lower than that of organic fluorophores and QDs, and they typically require excitation with a 980 nm laser and specialized, non-commercial instrumentation. Furthermore, their composition, often involving lanthanides, rare-earth elements, and transition metals, raises concerns about potential toxicity, limiting their suitability for diagnostic applications.

3.3.2. Applications.

Particle-based fluorescent POC technologies enable the detection of diverse medical targets, such as infectious and cardiac diseases, cancer biomarkers, and blood glucose levels.

In viral diagnostics, Xu *et al.* introduced fluorescent carbon dot–based silica (FCS) lateral flow strips for detecting the dengue virus NS1 antigen (Fig. 8A).[202] These test strips, read under UV light, demonstrated a detection limit 100 times lower than conventional gold nanoparticle (AuNP)-based strips, with excellent reproducibility and stability. Similarly, Guo *et al.* developed a fluorescent lateral flow immunoassay LFIA platform using UCNPs encapsulated in mesoporous silica (UCNPs@ $mSiO_2$) to simultaneously detect the spike (S) and nucleocapsid (N) proteins of SARS-CoV-2.[203] Coupled with a 5G-enabled fluorescent reader, the system achieved detection limits of 1.6 ng mL^{-1} for the S protein and 2.2 ng mL^{-1} for the N protein.

Beyond single-mode sensing, multimodal POC strategies have demonstrated superior performance by combining complementary signal outputs (colorimetric, fluorescent, and magnetic) to improve sensitivity, robustness, and resistance to interference. For example, Hu *et al.* reported a multimodal LFIA integrating colorimetric, fluorescent, and magnetic NPs, resulting in improved assay performance (Fig. 8B).[204] They demonstrated a dual-signal LFIA for Ebola virus detection using RNs@Au (QDs + gold) nanospheres, achieving rapid and
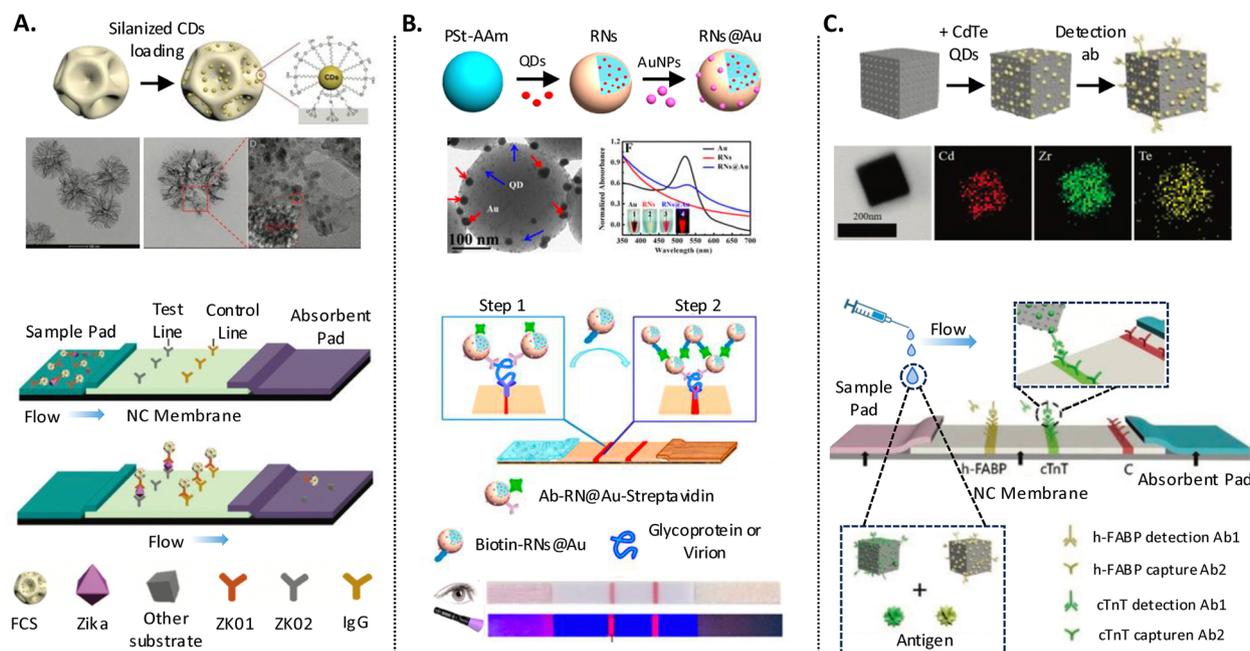

Fig. 8 (A). Schematic illustration of the synthetic procedures of CD embedded SiO$_2$ spheres and the TEM image of dendritic SiO$_2$ and HRTEM images of FCS spheres. Schematic representation of Zika NS1 protein detection using the iFCS-based lateral flow immunoassay. Reproduced with permission[202] copyright 2021 Royal Society of Chemistry. (B) Schematic illustration of the preparation of RNs@Au and corresponding characterization: TEM image of RNs@Au (blue and red arrows indicate QD and Au, respectively) and UV-vis absorption spectra of Au, RNs, and RNs@Au. Below: schematic illustration of EBOV detection using an enhanced RNs@Au-based test strip: the target was labeled with Ab−RNs@Au−SA and captured by the test line of antibody to glycoprotein *via* antigen−antibody reaction. In the second step, biotin−RNs@ Au solution was applied to the sample pad. Biotin−RNs@Au were adhered to the test line by Ab−RNs@Au−SA *via* biotin−SA affinity, and then a network of RNs@Au can form on the test line through multivalent interactions of biotin−SA, in which a darker and brighter signal was obtained. Reproduced with permission[204] copyright 2017 American Chemical Society. (C) Experimental process for the preparation of ZrMOF@CdTe−Ab conjugates and HTEM-mapping image. Corresponding schematic representation of the LFA for cTnT and h-FABP detection. Reproduced with permission[208] copyright 2021 Royal Society of Chemistry.

5618 | *J. Mater. Chem. C*, 2026, **14**, 5607−5628

This journal is © The Royal Society of Chemistry 2026

sensitive analysis of spiked samples within 20 minutes, detectable both visually and *via* fluorescence.

Fluorescent nanoparticle-based POC systems have also shown promise for cancer diagnostics. Liang *et al.* used aptamer-conjugated SiNPs coated with QDs on graphene oxide surfaces.[205] Fluorescence is quenched by FRET but restored in the presence of target cancer cells. By changing aptamers and quantum dot colours, different cancer cells can be detected simultaneously with one light source. Likewise, Jimenez *et al.* developed a biosensor using gold-coated superparamagnetic nanomaghemite (AuMNPs) functionalized with DNA probes targeting the HPV-16 E6 oncogene.[206] Detection relies on binding viral DNA and signalling *via* peptide-modified QDs. Tested for specificity against other viruses, it was successfully applied to patient samples and confirmed by PCR. This system offers a low-cost, sensitive alternative to traditional PCR for HPV detection, offering a low-cost alternative for HPV-related cancer diagnostics.

In the field of cardiovascular diseases (CVDs), Y. Fan Shi *et al.* developed a magnetic multilayer lanthanide MOF-based sensor (MagMOF) designed for the simultaneous detection of acute myocardial infarction (AMI) biomarkers such as CK-MB, troponin I (cTnI), and myoglobin (Mb), along with aspirin, a common treatment.[207] Using a layer-by-layer assembly strategy, this hybrid nanosensor integrates antibodies and mRNA probes with MagMOF nanoballs, enabling highly sensitive detection within clinically relevant ranges. The platform offers rapid, stable, and multiplexed detection, showing strong potential for POC AMI diagnosis and therapeutic monitoring. Similarly, Jian Zou *et al.* studied a ZrMOF-based lateral flow assay using fluorescent ZrMOF@CdTe nanoparticles that enables rapid (8 min) and multiplexed detection of AMI biomarkers like h-FABP and cTnT (Fig. 8C).[208] With a visual detection limit of $1 \mu g L^{-1}$ for h-FABP, it is simple, low-cost, and effective for POC use in serum samples.

Fluorescent POC sensing has also advanced in continuous glucose monitoring (CGM). To address limitations in traditional electrochemical CGMs, including instability, interference, and electrode degradation, a nanodiamond-boronic hydrogel system has been developed for integration into porous microneedles.[209] These highly photostable and biocompatible nanodiamonds emit fluorescence in response to glucose levels. The hydrogel-based sensor offers long-term signal stability *in vivo*, as shown in animal models, and avoids common issues of electrochemical sensors. This proof-of-concept marks a promising step toward reliable, minimally invasive CGM using fluorescence technology.

Magnetic and fluorescent nanocomposites have further expanded the capabilities of optical POC systems. Tombelli *et al.* reported a compact fluorescence-based immunoassay device using disposable plastic chips for multi-analyte detection of immunosuppressants.[210] The chip integrates ten parallel microchannels, on-chip microfluidics, and photodiodes for direct fluorescence readout. Submicron fluorescent magnetic particles accelerate the reaction kinetics through magnetic concentration while enhancing sensitivity through optical labelling. Reusability and integration with microdialysis

sampling allowed continuous therapeutic monitoring for up to 48 hours, providing valuable pharmacokinetic insights.

Combined with MoS_2 and Eu^{3+}, QDs were employed to develop a ratiometric fluorescent probe for sensitive tetracycline (TC) detection in biological samples. The method relies on energy transfer between MoS_2 QDs and Eu–TC complexes, enhancing luminescence at 620 nm while quenching at 470 nm, enabling ratiometric detection (F_{620}/F_{470}). It offers a 10 nM–60 μM linear range, 2 nM detection limit, high recovery (94.4–108.4%), and precision ($<5.36\%$ RSD). A smartphone-based platform enables visual, portable quantification with a 0.05 μM detection limit, providing a fast, low-cost solution for antibiotic monitoring.[211]

Beyond biomedical applications, nanoparticle-based POC platforms are also showing remarkable potential in environmental monitoring. Liang *et al.* developed a multicolor fluorescent probe for visual and smartphone-assisted detection of common water additives.[212] The ratiometric system combines blue-emitting CDs and red-emitting gold NCs, producing visible color changes under UV light upon exposure to analytes such as ascorbic acid, sodium sulfite, and hydrogen peroxide. The probe exhibited high selectivity, rapid response (<5 min), and excellent performance in real water samples, demonstrating the versatility of fluorescent POC technologies for on-site environmental assessment.

Jin *et al.* developed a multiplex paper-based aptasensor for POC water quality monitoring, integrating UCNPs and specific aptamers for the simultaneous detection of multiple contaminants, including pathogens (Salmonella), toxins (ochratoxin A, microcystin-LR), and heavy metals (Hg^{2+}, Pb^{2+}).[213] The system achieves high sensitivity, with detection limits as low as 115 CFU mL^{-1} for Salmonella, and 4 nM are read using a compact, smartphone-based device, enabling portable, rapid (≤ 30 min), and instrument-free analysis. The platform showed high specificity and minimal cross-reactivity, and has been successfully tested in real water samples (tap and pond water), making it a promising tool for decentralized and field-based water quality assessment.

3.4. Comparative analysis

Table 1 summarizes the principal characteristics of the fluorescent probe classes discussed in Sections 3.1–3.3, providing a comparative overview of performance-related parameters relevant to fluorescence-based POC applications, including sensitivity, photostability, biocompatibility, and practical advantages and limitations. Across the different probe categories, engineered nanomaterials generally exhibit higher signal robustness and photostability than organic fluorophores and fluorescent proteins, which can be advantageous for applications requiring high sensitivity or prolonged signal acquisition. However, superior optical performance does not necessarily correlate with biocompatibility, regulatory acceptance, or translational suitability. For example, QDs represent the highest-performing class in terms of optical properties, achieving detection limits down to the aM range while maintaining exceptional photostability and narrow, size-tunable emission spectra. These features

This journal is © The Royal Society of Chemistry 2026

J. Mater. Chem. C, 2026, **14**, 5607–5628 | **5619**

Table 1 Overview of fluorescent probes used in POC technologies

Probe type	Sensitivity	Photostability	Biocompatibility	Key advantages	Limitations	Ref.
Organic fluorophores	Moderate (nM)	Moderate to low	Good	Small size; well-known photophysics	Photobleaching; narrow Stokes shift	81 and 214–216
Fluorescent proteins	Moderate (nM)	Limited	Excellent	Genetic encoding; intracellular targeting	Photobleaching; narrow spectral range	48, 217 and 218
MNPs	High (fM)	Excellent	Variable	Plasmonic fluorescence enhancement	Potential toxicity; less explored	162, 164 and 219
MOFs	Moderate–high (pM)	Good	Generally good	High loading capacity; multifunctionality	Stability issues in biological media	156 and 220
SiNPs	Moderate (nM)	Good	Good	Biocompatible; easy surface modification	Potential aggregation	120, 170, 173 and 183
QDs	Very high (aM)	Excellent	Moderate (toxicity concerns)	Bright, narrow tunable emission spectra	Heavy metal toxicity; regulatory issues	191 and 192
Carbon-based NPs	Moderate–high (pM)	Very good	Excellent	Low toxicity; versatile excitation/emission	Lower brightness than QDs	157, 190 and 191
UCNPs	Moderate–high (pM)	Excellent	Good	NIR excitation, low autofluorescence	Lower quantum yield; complex synthesis	198, 199 and 221

enable highly multiplexed detection and prolonged signal acquisition, making QDs attractive for ultra-trace and multi-analyte analysis. Nevertheless, their heavy-metal composition raises cytotoxicity and regulatory concerns that currently limit widespread clinical translation, highlighting the gap that can exist between analytical performance and practical implementability.[222]

MNPs offer an alternative route to high analytical sensitivity, frequently reaching fM detection levels through plasmon-enhanced fluorescence mechanisms. Their ability to amplify emission signals and improve signal-to-noise ratios supports their use in rapid immunoassays and lateral-flow-based POC platforms. At the same time, performance strongly depends on surface chemistry, particle architecture, and probe–particle spacing, which can introduce variability and reproducibility challenges when transitioning from laboratory prototypes to standardized diagnostic formats.[162,164]

MOFs, carbon-based NPs, and UCNPs represent platforms that seek to balance optical performance with biocompatibility and functional versatility. MOFs offer high loading capacity and multifunctionality, enabling integrated analyte recognition and signal transduction, although their stability in biological fluids remains a critical limitation for long-term operation in complex matrices.[156,220] Carbon-based NPs, including carbon dots and graphene derivatives, address several limitations associated with metal-containing probes by providing enhanced biocompatibility and chemical stability while maintaining sufficient sensitivity for most clinically relevant POC assays, despite lower brightness than QDs.[157,190] UCNPs introduce a distinct optical advantage by enabling near-infrared excitation, which reduces background autofluorescence and improves tissue penetration. However, their relatively low quantum yield and the requirement for specialized excitation sources complicate integration into low-cost, miniaturized diagnostic platforms.[199]

Organic fluorophores and fluorescent proteins remain highly relevant for applications prioritizing simplicity, genetic encoding capability, or intracellular monitoring.[223] Organic fluorophores benefit from well-characterized photophysics, straightforward functionalization, and compatibility with disposable, low-cost devices,[81,214–216] but their susceptibility to photobleaching and limited sensitivity constrain their use in long-term or ultra-low-concentration detection. Fluorescent proteins provide unmatched specificity for intracellular sensing and genetically encoded biosensing strategies, yet their limited photostability and dependence on biological expression systems restrict their applicability in cell-free or disposable POC devices.[48,217,218]

Beyond analytical metrics, practical considerations play a decisive role in probe selection. Highly sensitive nanoparticle-based POC systems often require complex synthesis protocols, surface functionalization, and advanced instrumentation, whereas molecular probes are generally easier to integrate into portable and cost-effective devices. Overall, the discussion in Sections 3.1–3.3 and the comparison in Table 1 underscore that the selection of fluorescent probes for POC technologies is inherently application-dependent and requires a careful balance between optical performance, biocompatibility, stability, and implementation constraints.

4. Challenges and future perspectives

Fluorescence-based POC devices enable rapid, sensitive, and portable analyses across diverse application domains, including diagnostics, therapeutic monitoring, environmental analysis, and wearable systems (Fig. 9). However, despite these advantages, several challenges must still be addressed to unlock their full translational potential. Critical issues include probe and signal stability, reduced sensitivity in complex matrices, limited standardization, and the need for more robust, user-friendly readout systems. These aspects are discussed in detail below.

4.1. Limitations and challenges of fluorescence-based POC technologies

Despite recent progress, several limitations hinder the widespread adoption and long-term performance of fluorescence-based POC systems.

A key limitation of fluorescent probes is their susceptibility to environmental conditions, as factors such as temperature, pH, ionic strength, and solvent polarity can significantly affect

5620 | J. Mater. Chem. C, 2026, 14, 5607–5628

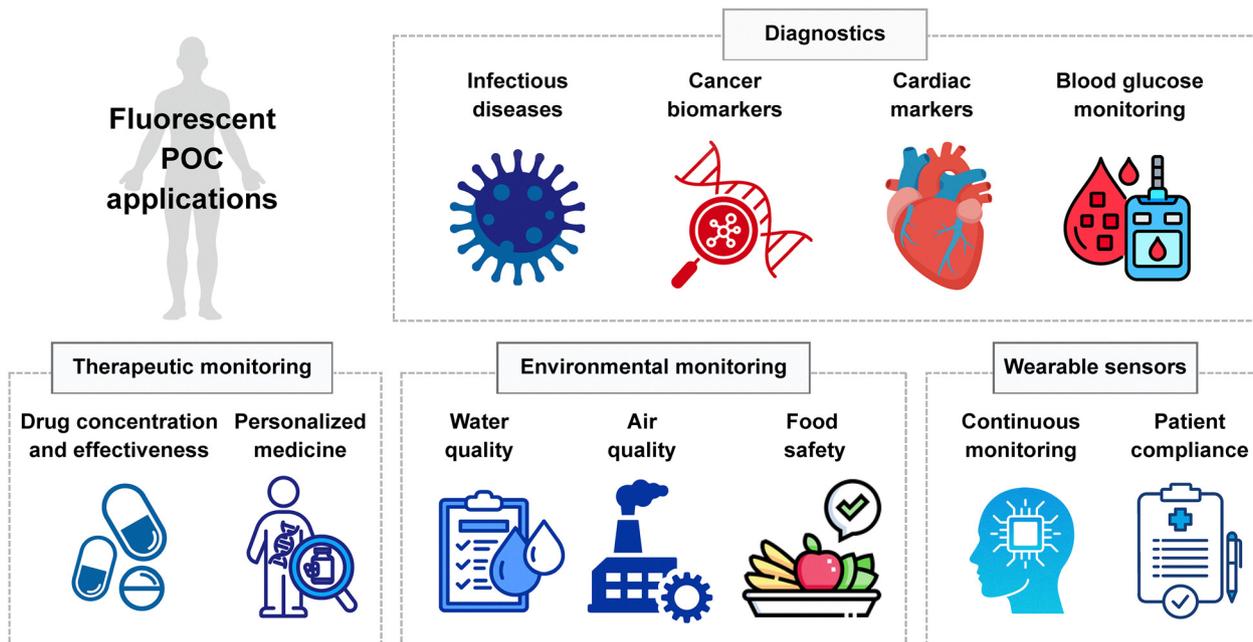This journal is © The Royal Society of Chemistry 2026

Fig. 9 General applications of fluorescence-based POC devices.

both quantum yield and emission spectra. These factors cause instability and impair measurement reproducibility, especially in uncontrolled field circumstances, such as complex media (human serum, whole blood, urine, saliva, etc.).[224] Thus, while fluorescence-enhancing systems have been widely explored to improve biosensor sensitivity, their translation to clinical practice remains limited, with few systems tested in biologically complex fluids or validated in real clinical conditions.[225,226] Moreover, the same labelling processes frequently require laborious procedures for attaching fluorescent tags to biomolecules like proteins. This step is mandatory for the detection of analytes lacking intrinsic fluorescence; however, its performance may be adversely affected by interfering substances within the sample matrix, potentially compromising signal reliability and analytical accuracy. To minimize procedural steps and their associated challenges, several studies have focused on integrating microfluidic systems capable of performing sequential operations, including sample separation or filtration, reagent mixing, target labelling, and washing, to streamline sample preparation and improve assay efficiency.[227–229]

Photobleaching remains another major limitation, resulting in progressive signal decay during repeated or prolonged excitation. Reactive oxygen species or radical intermediates commonly contribute to photodegradation, limiting time-lapse detection and reducing suitability for long-term monitoring. Furthermore, matrix-related effects such as quenching by biomolecules (e.g., proteins, lipids, and nucleic acids) and high background autofluorescence further complicate measurements. These interferences lower signal-to-noise ratios and frequently demand complex sample pretreatment or filtration processes.

Beyond technical constraints, standardization of measurement protocols, validation procedures, and quality assurance measures remains critical for widespread adoption of these technologies. The development of reference standards and inter-laboratory comparison programs will support regulatory acceptance and commercial deployment. The integration of fluorescence-based sensors with emerging technologies, including artificial intelligence, blockchain for data integrity, and Internet of Things (IoT) platforms, promises to enhance the capabilities and applications of these monitoring systems.[230,231] Advanced data analytics and machine learning algorithms will improve the interpretation of complex fluorescence signatures and enable predictive monitoring capabilities.

Finally, regulatory validation and clinical translation of fluorescence-based POC devices require rigorous performance benchmarking, repeatability investigations, and safety assessments. These steps are extremely time-consuming and expensive, especially when applied to multiplexed or nanomaterial-based platforms, impeding their road to market and limiting acceptance in resource-constrained environments.

Overcoming these constraints will necessitate collaborative work in materials science, optical engineering, microfluidics, and artificial intelligence to create next-generation POC systems that are robust, scalable, and comply with international diagnostic standards.

The development and validation of emerging microfluidic and POC fluorescence platforms critically depend on established fluorescence-based reference techniques. Flow cytometry, plate-reader fluorescence assays, and conventional fluorescence microscopy serve as gold standards to benchmark sensitivity, specificity, dynamic range, and reproducibility.[232]

Flow cytometry offers high-throughput multiparametric analysis using well-established fluorescence signals, making it a reliable reference technique for validating novel microfluidic devices. Relying on such established methodologies helps ensure that emerging platforms meet rigorous analytical standards and

This journal is © The Royal Society of Chemistry 2026

J. Mater. Chem. C, 2026, 14, 5607–5628 | 5621

supports their translational development. Recent studies have shown that high-throughput fluorescence lifetime imaging flow cytometry can acquire detailed lifetime and intensity images at rates that overcome conventional speed limitations, improving the discrimination of cellular subpopulations in dynamic biological settings.[233] In parallel, work on the immunomagnetic separation of B-type acute lymphoblastic leukemia blast cells from bone marrow has used flow cytometry to validate capture efficiency and benchmark microfluidic chip performance, highlighting how combining targeted separation strategies with established cytometric readouts enables quantitative evaluation of device performance.[234]

From this perspective, flow cytometry serves as an effective bridge between traditional fluorescence-based methods and emerging point-of-care technologies.

4.2. Emerging trends and novel POC technologies

Fluorescence-based POC technologies are rapidly evolving through the development of novel materials, advanced detection strategies, and improved system integration.[235,236]

One of the main drivers of innovation is the emergence of next-generation fluorescent probes with improved brightness, photostability, and selectivity compared to traditional organic dyes. QDs with their size-tunable emission and exceptional photostability, allow highly sensitive and multiplexed biomarker detection with negligible spectral overlap. Their broad absorption and narrow emission profiles make them ideal for high-content, multi-analyte assays.

In parallel, AIE fluorophores have emerged as a complementary class of probes. Unlike conventional dyes that suffer from fluorescence quenching upon aggregation, AIE molecules become highly emissive upon aggregation, which significantly reduces background noise and enhances the signal-to-noise ratio. This property is particularly beneficial for detecting low-abundance targets in complex biological samples.[237]

Another key technological advancement is the incorporation of smartphone-based fluorescence readers, leveraging the widespread availability of mobile devices to create portable, cost-effective, and user-friendly diagnostic platforms.[16,237] These systems often combine compact optical components with sophisticated image processing algorithms, facilitating real-time quantification and data sharing, which is critical for remote healthcare and telemedicine applications.

Moreover, microfluidics and LoC technologies are increasingly integrated with fluorescent detection to automate sample handling and reduce assay times, enhancing the practicality of POC testing in diverse settings.[238]

The use of AI and machine learning algorithms to analyse fluorescence signals is also emerging as a powerful tool to improve diagnostic accuracy and interpret complex data patterns.[239] AI algorithms process diverse fluorescence data types including intensity-based signals, spectral profiles, fluorescence lifetime measurements, and imaging datasets.[240]

Key AI roles encompass feature extraction, noise reduction, classification, regression, and multiplexed target discrimination.[241] For example, convolutional neural networks (CNNs) excel in analyzing fluorescence microscopy images for cell identification and sorting, while machine learning classifiers enhance spectral unmixing for complex multiplex assays.[242]

These AI-driven approaches yield measurable gains such as improved sensitivity, increased robustness against background interference, reduced analysis time, and enhanced multiplexing capacity. As AI methods evolve, they are expected to further expand the capabilities and clinical utility of fluorescence-based POC diagnostics.

On the other hand, the transition from proof-of-concept prototypes to clinically deployable devices remains a considerable challenge.[243] For example, lateral flow assays incorporating fluorescent NPs have reached commercial availability, offering improved sensitivity over traditional colorimetric tests.[244] Conversely, novel microfluidic platforms integrating fluorescence lifetime measurements often remain at early developmental stages, requiring further validation in clinical matrices to confirm robustness.[245]

Technologies at more advanced stages often feature durable materials, optimized probe chemistries, and fully integrated microfluidic systems that have been validated under realistic sample conditions, demonstrating scalability and adherence to regulatory standards. In contrast, earlier-stage platforms mainly focus on proof-of-principle demonstrations or novel sensing modalities, lacking extensive validation in clinically relevant matrices.[246] Recognizing these developmental distinctions is essential to prioritize research directions, inform investment strategies, and set realistic timelines for clinical adoption. Additionally, recent advances in AI-assisted fluorescence analysis have shown considerable promise for improving diagnostic accuracy, though they are still under evaluation for robustness and feasibility in real-world deployment.[247] Clearly distinguishing between these stages is critical to accelerating translation and ensuring that fluorescence-based innovations fulfil the clinical and operational requirements of decentralized healthcare.

5. Conclusions

This review provides a comprehensive overview of fluorescence-based technologies and their evolution into advanced applications in POC diagnostic technologies. It analyses the fundamental principles and instrumentation of key fluorescence techniques, including spectroscopy, microscopy, time-resolved fluorescence, and FLIM, highlighting their increasing sensitivity, spatial and temporal resolution, and multiplexing capabilities. Moreover, this review presents a detailed analysis of the main classes of fluorescent probes, such as organic fluorophores, fluorescent proteins, QDs, and UCNPs, discussing their unique photophysical features and suitability for portable diagnostic formats. This review also explores the broad range of POC applications enabled by these systems, spanning clinical diagnostics, therapeutic drug monitoring, environmental analysis and wearable biosensors. Collectively, fluorescence-based POC devices stand out for their portability, rapid detection capability, analytical sensitivity and suitability for use in resource-limited environments.

Looking ahead, the future of fluorescence-based technologies in POC diagnostics and monitoring appears highly promising. The integration of smart biosensors, artificial intelligence, and microfluidic architectures is transforming how biomarkers are detected and quantified, in real time and with high specificity. There is a clear trend toward more portable, customizable, and user-friendly devices that enable continuous, minimally invasive monitoring and seamless connectivity to digital healthcare infrastructures. Advances in miniaturization, alongside the development of more stable, biocompatible, and near-infrared-emitting probes, are expected to enhance their translational potential across clinical and environmental settings.

However, key challenges remain. Regulatory approval, large-scale clinical validation, and robust standardization are essential to ensure reliability and reproducibility. Overcoming these barriers will require sustained collaboration between materials scientists, optical engineers, clinicians, and policymakers. With continued interdisciplinary progress, fluorescence-based POC systems have the potential to redefine personalized and preventive healthcare, expanding diagnostic access and improving outcomes on a global scale.

Author contributions

Conceptualization and original outline: A. C.; conceptualization and manuscript restructuring: L. L. d. M., M. C.-M., E. S., and G. V.; data curation: H. I., F. C., S. F., V. O., G. G., and A. C.; funding acquisition: Gi. Gi., A. C., and L. L. d. M.; project administration: L. L. d. M.; resources: Gi. Gi., A. C., and L. L. d. M.; supervision: L. L. d. M.; visualization: M. C.-M. and L. L. d. M.; writing – original draft: M. C.-M., E. S., G. V., A. C., H. I., F. C., S. F., V. O., and G. G.; writing – review and editing: M. C.-M., E. S., G. V., A. C., F. C., and L. L. d. M.

Conflicts of interest

There are no conflicts to declare.

Data availability

No new data were generated or analyzed in this study. Data sharing is not applicable.

Acknowledgements

References

1 S.-H. Huang, Y.-H. Huang and L.-C. Chiu, *Int. J. Syst. Sci.-Oper. Logist.*, 2024, 2374968.

2 B. Heidt, W. F. Siqueira, K. Eersels, H. Diliën, B. Van Grinsven, R. T. Fujiwara and T. J. Cleij, *Biosensors*, 2020, DOI: 10.3390/BIOS10100133.

3 K. Lakshmanan and B. M. Liu, *Diagnostics*, 2025, 123.

4 T. S. Pillay, A. I. Khan and S. Yenice, *Clin. Chim. Acta*, 2025, 120341.

5 Y. Liu, X. Zhao, M. Liao, G. Ke and X.-B. Zhang, *Sens. Diagn.*, 2024, **3**, 1789–1806.

6 A. Teymur, I. Hussain, C. Tang, R. Saxena, D. Erickson and T. Wu, *Micromachines*, 2025, **16**, 156.

7 D. Geißler, L. J. Charbonnière, R. F. Ziessel, N. G. Butlin, H. Löhmannsröben and N. Hildebrandt, *Angew. Chem., Int. Ed.*, 2010, **49**, 1396–1401.

8 R. B. Sekar and A. Periasamy, *J. Cell Biol.*, 2003, 629–633.

9 J. Chu, A. Ejaz, K. M. Lin, M. R. Joseph, A. E. Coraor, D. A. Drummond and A. H. Squires, *Nat. Nanotechnol.*, 2024, **19**, 1150–1157.

10 J. Aich, S. Singh, S. Chandrashekhar, V. Srivastav, S. Devarajan and S. Basu, in *Smart Diagnostics for Neurodegenerative Disorders*, Elsevier, 2024, pp. 179–196.

11 F. Shalileh, N. Shamani, M. Golbashy, M. Dadmehr and M. Hosseini, *Nanotechnology*, 2025, **36**, 052002.

12 Y. Xie, L. Dai and Y. Yang, *Biosens. Bioelectron. X*, 2022, 100109.

13 H. Wang, Q. Li, P. Alam, H. Bai, V. Bhalla, M. R. Bryce, M. Cao, C. Chen, S. Chen, X. Chen, Y. Chen, Z. Chen, D. Dang, D. Ding, S. Ding, Y. Duo, M. Gao, W. He, X. He, X. Hong, Y. Hong, J. J. Hu, R. Hu, X. Huang, T. D. James, X. Jiang, G. I. Konishi, R. T. K. Kwok, J. W. Y. Lam, C. Li, H. Li, K. Li, N. Li, W. J. Li, Y. Li, X. J. Liang, Y. Liang, B. Liu, G. Liu, X. Liu, X. Lou, X. Y. Lou, L. Luo, P. R. McGonigal, Z. W. Mao, G. Niu, T. C. Owyong, A. Pucci, J. Qian, A. Qin, Z. Qiu, A. L. Rogach, B. Situ, K. Tanaka, Y. Tang, B. Wang, D. Wang, J. Wang, W. Wang, W. X. Wang, W. J. Wang, X. Wang, Y. F. Wang, S. Wu, Y. Wu, Y. Xiong, R. Xu, C. Yan, S. Yan, H. B. Yang, L. L. Yang, M. Yang, Y. W. Yang, J. Yoon, S. Q. Zang, J. Zhang, P. Zhang, T. Zhang, X. Zhang, X. Zhang, N. Zhao, Z. Zhao, J. Zheng, L. Zheng, Z. Zheng, M. Q. Zhu, W. H. Zhu, H. Zou and B. Z. Tang, *Aggregation-Induced Emission (AIE), Life and Health*, American Chemical Society, 2023, DOI: 10.1021/acsnano.3c03925.

14 W. Chen, H. Guan, Y. Lu, G. Zeng, D. Gu, K. Guo, C. Jiang and H. Liu, *Aggregate*, 2025, e70008.

This journal is © The Royal Society of Chemistry 2026

J. Mater. Chem. C, 2026, **14**, 5607–5628 | **5623**

15 D. Zhang and Q. Liu, *Biosens. Bioelectron.*, 2016, **75**, 273–284.

16 J. F. Bergua, R. Álvarez-Diduk, A. Idili, C. Parolo, M. Maymó, L. Hu and A. Merkoçi, *Anal. Chem.*, 2022, **94**, 1271–1285.

17 K. E. Sapsford, L. Berti and I. L. Medintz, in *Wiley Encyclopedia of Chemical Biology*, Wiley, 2008, pp. 1–23.

18 S. Deshayes and G. Divita, *Prog. Mol. Biol. Transl. Sci*, 2013, **113**, 109–143.

19 M. J. Sanderson, I. Smith, I. Parker and M. D. Bootman, *Cold Spring Harb. Protoc.*, 2014, **2014**, pdb.top071795.

20 J. R. Lakowicz, *Principles of fluorescence spectroscopy*, Springer, 2006.

21 D.-E. Zacharioudaki, I. Fitilis and M. Kotti, *Molecules*, 2022, **27**, 4801.

22 H. H. Telle and Á. G. Ureña, *Laser Spectroscopy and Laser Imaging*, CRC Press, 2018.

23 M. Y. Berezin and S. Achilefu, *Chem. Rev.*, 2010, **110**, 2641–2684.

24 D. J. S. Birch, Y. Chen and O. J. Rolinski, in *Photonics*, Wiley, 2015, pp. 1–58.

25 S. Nagl, M. Schaeferling and O. S. Wolfbeis, *Microchim. Acta*, 2005, **151**, 1–21.

26 Y. Fu, T. Liu, H. Wang, Z. Wang, L. Hou, J. Jiang and T. Xu, *J. Sci.: Adv. Mater. Devices*, 2024, **9**, 100694.

27 S. Dolai, S. K. Bhunia, S. Rajendran, V. UshaVipinachandran, S. C. Ray and P. Kluson, *Crit. Rev. Solid State Mater. Sci.*, 2021, **46**, 349–370.

28 G. Feng, G.-Q. Zhang and D. Ding, *Chem. Soc. Rev.*, 2020, **49**, 8179–8234.

29 H. Wang, J. Tang, X. Wan, X. Wang, Y. Zeng, X. Liu and D. Tang, *Anal. Chem.*, 2024, 15503.

30 D. P. O'Neal, M. A. Meledeo, J. R. Davis, B. L. Ibey, V. A. Gant, M. V. Pishko and G. L. Cote, *IEEE Sens. J.*, 2004, **4**, 728–734.

31 A. Kumar, V. S. Goudar, B. K. Nahak, P. Tsai, H. Lin and F. Tseng, *Small*, 2024, 2307955.

32 H. Iuele, S. Forciniti, V. Onesto, F. Colella, A. C. Siciliano, A. Chandra, C. Nobile, G. Gigli and L. L. del Mercato, *ACS Appl. Mater. Interfaces*, 2024, 55071.

33 G. Grasso, S. Forciniti, V. Onesto, L. Pierantoni, D. Caballero, E. D'Amone, G. Gigli, R. L. Reis, J. M. Oliveira and L. L. del Mercato, *Biosens. Bioelectron.*, 2025, **283**, 117481.

34 G. Grasso, V. Onesto, S. Forciniti, E. D'Amone, F. Colella, L. Pierantoni, V. Famà, G. Gigli, R. L. Reis, J. M. Oliveira and L. L. del Mercato, *Biodes. Manuf*, 2024, **7**, 292–306.

35 M. H. Gehlen, *J. Photochem. Photobiol., C*, 2020, **42**, 100338.

36 S. E. Webber, *Photochem. Photobiol.*, 1997, **65**, 33–38.

37 B. I. Ipe, K. Yoosaf and K. G. Thomas, *J. Am. Chem. Soc.*, 2006, **128**, 1907–1913.

38 Q. Tan, R. Zhang, G. Zhang, X. Liu, F. Qu and L. Lu, *Anal. Bioanal. Chem.*, 2020, **412**, 1317–1324.

39 E. A. Specht, E. Braselmann and A. E. Palmer, *Annu. Rev. Physiol.*, 2017, **79**, 93–117.

40 M. H. Jennison and A. F. Morgan, *Tubercle*, 1950, **31**, 84–87.

41 S. Prasad, A. Chandra, M. Cavo, E. Parasido, S. Fricke, Y. Lee, E. D'Amone, G. Gigli, C. Albanese, O. Rodriguez and L. L. del Mercato, *Nanotechnology*, 2021, **32**, 062001.

42 F. Alemanno, M. Cavo, D. Delle Cave, A. Fachechi, R. Rizzo, E. D'Amone, G. Gigli, E. Lonardo, A. Barra and L. L. del Mercato, *Proc. Natl. Acad. Sci. U. S. A.*, 2023, e2122352120.

43 F. Carnevali, S. Forciniti, V. Onesto, A. C. Siciliano, H. Iuele, G. Grasso, A. F. da Cruz, I. Serra, N. Depalma, S. D'Ugo, P. Piscitelli, M. G. Spampinato, G. Gigli, C. Camargo de Oliveira and L. L. del Mercato, *Adv. Ther.*, 2024, 2400351.

44 R. Kasprowicz, R. Suman and P. O'Toole, *Int. J. Biochem. Cell Biol.*, 2017, **84**, 89–95.

45 H. Yokota, *Biochim. Biophys. Acta Gen. Subj.*, 1864, **2020**, 129362.

46 A. L. Robson, P. C. Dastoor, J. Flynn, W. Palmer, A. Martin, D. W. Smith, A. Woldu and S. Hua, *Front. Pharmacol.*, 2018, **9**, 1–8.

47 S. J. Sahl, S. W. Hell and S. Jakobs, *Nat. Rev. Mol. Cell Biol.*, 2017, **18**, 685–701.

48 B. C. Campbell, M. G. Paez-Segala, L. L. Looger, G. A. Petsko and C. F. Liu, *Nat. Methods*, 2022, **19**, 1612–1621.

49 S. Y. Kim, Y. Arai, T. Tani, H. Takatsuka, Y. Saito, T. Kawashima, S. Kawakami, A. Miyawaki and T. Nagai, *Microscopy*, 2017, **66**, 110–119.

50 N. V. dos Santos, C. F. Saponi, T. M. Ryan, F. L. Primo, T. L. Greaves and J. F. B. Pereira, *Int. J. Biol. Macromol.*, 2020, **164**, 3474–3484.

51 J. W. Lichtman and J. A. Conchello, *Nat. Methods*, 2005, **2**, 910–919.

52 W. Justyna, *Curr Protoc Cytom*, 2017, **176**, 139–148.

53 S. P. Poland, N. Krstajić, S. Coelho, D. Tyndall, R. J. Walker, V. Devauges, P. E. Morton, N. S. Nicholas, J. Richardson, D. D.-U. Li, K. Suhling, C. M. Wells, M. Parsons, R. K. Henderson and S. M. Ameer-Beg, *Opt. Lett.*, 2014, **39**, 6013.

54 V. I. Shcheslavskiy, M. V. Shirmanova, K. S. Yashin, A. C. Rück, M. C. Skala and W. Beker, *J. Biophotonics*, 2025, **18**(12), e202400450.

55 R. Datta, T. M. Heaster, J. T. Sharick, A. A. Gillette and M. C. Skala, *J. Biomed. Opt.*, 2020, **25**, 1.

56 J. Bleeker, A. P. Kahn, L. M. Baumgartner, F. C. Grozema, D. A. Vermaas and W. F. Jager, *ACS Sens.*, 2023, **8**, 2050–2059.

57 K. Suhling, L. M. Hirvonen, W. Becker, S. Smietana, H. Netz, J. Milnes, T. Conneely, A. Le Marois, O. Jagutzki, F. Festy, Z. Petrášek and A. Beeby, *Nucl. Instrum. Methods Phys. Res. A*, 2019, **942**, 162365.

58 W. R. Algar, N. Hildebrandt, S. S. Vogel and I. L. Medintz, *Nat. Methods*, 2019, **16**, 815–829.

59 R. Datta, T. M. Heaster, J. T. Sharick, A. A. Gillette and M. C. Skala, *J. Biomed. Opt.*, 2020, **25**, 1.

60 T. Hinsdale, C. Olsovsky, J. J. Rico-Jimenez, K. C. Maitland, J. A. Jo and B. H. Malik, *Biomed. Opt. Express*, 2017, **8**, 1455.

61 N. Oleksiievets, C. Mathew, J. C. Thiele, J. I. Gallea, O. Nevskyi, I. Gregor, A. Weber, R. Tsukanov and J. Enderlein, *Nano Lett.*, 2022, **22**, 6454–6461.

62 J. E. Phipps, J. Bec and L. Marcu, *Multimodality Imaging*, Springer Singapore, Singapore, 2020, pp. 153–171.

63 A. Alfonso-Garcia, J. Bec, S. Sridharan Weaver, B. Hartl, J. Unger, M. Bobinski, M. Lechpammer, F. Girgis, J. Boggan and L. Marcu, *J. Biophotonics*, 2020, **13**, e201900108.

5624 | *J. Mater. Chem. C*, 2026, **14**, 5607–5628

This journal is © The Royal Society of Chemistry 2026

64 A. Alfonso-Garcia, J. Bec, B. Weyers, M. Marsden, X. Zhou, C. Li and L. Marcu, *J. Biophotonics*, 2021, **14**, e202000472.

65 A. P. Demchenko, *Introduction to fluorescence sensing*, 2009, 65–118.

66 R. Kang, L. Talamini, E. D'Este, B. M. Estevao, L. De Cola, W. Klopper and F. Biedermann, *Chem. Sci.*, 2021, **12**, 1392–1397.

67 S. Yang, Y. Zhan, W. Shou, L. Chen, Z. Lin and L. Guo, *ACS Appl. Bio Mater.*, 2021, **4**, 6065–6072.

68 J. Zhang, S. Shikha, Q. Mei, J. Liu and Y. Zhang, *Microchim. Acta*, 2019, **186**, 1–21.

69 X. Gao, H. Xu, M. Baloda, A. S. Gurung, L.-P. Xu, T. Wang, X. Zhang and G. Liu, *Biosens. Bioelectron.*, 2014, **54**, 578–584.

70 F. G. Prendergast and K. G. Mann, *Biochemistry*, 1978, **17**, 3448–3453.

71 H. Chen, J. Yu, X. Men, J. Zhang, Z. Ding, Y. Jiang, C. Wu and D. T. Chiu, *Angewandte Chemie*, 2021, **133**, 12114–12119.

72 N. T. Harrison, D. R. Baigent, I. D. W. Samuel, R. H. Friend, A. C. Grimsdale, S. C. Moratti and A. B. Holmes, *Phys. Rev. B*, 1996, **53**, 15815.

73 Z. Li, X. Zhao, C. Huang and X. Gong, *J. Mater. Chem. C Mater.*, 2019, **7**, 12373–12387.

74 S. Singh, A. Dhawan, S. Karhana, M. Bhat and A. K. Dinda, *Micromachines*, 2020, **11**, 1058.

75 M. Cordeiro, F. Ferreira Carlos, P. Pedrosa, A. Lopez and P. V. Baptista, *Diagnostics*, 2016, **6**, 43.

76 B. Della Ventura, M. Gelzo, E. Battista, A. Alabastri, A. Schirato, G. Castaldo, G. Corso, F. Gentile and R. Velotta, *ACS Appl. Mater. Interfaces*, 2019, **11**, 3753–3762.

77 Q. Liu, Q. Sun, J. Shen, H. Li, Y. Zhang, W. Chen, S. Yu, X. Li and Y. Chen, *Coord. Chem. Rev.*, 2023, **482**, 215078.

78 P. P. Pompa, R. Chiuri, L. Manna, T. Pellegrino, L. L. del Mercato, W. J. Parak, F. Calabi, R. Cingolani and R. Rinaldi, *Chem. Phys. Lett.*, 2006, **417**, 351–357.

79 K. Tomimuro, K. Tenda, Y. Ni, Y. Hiruta, M. Merkx and D. Citterio, *ACS Sens.*, 2020, **5**, 1786–1794.

80 L. Wu, C. Huang, B. P. Emery, A. C. Sedgwick, S. D. Bull, X.-P. He, H. Tian, J. Yoon, J. L. Sessler and T. D. James, *Chem. Soc. Rev.*, 2020, **49**, 5110–5139.

81 X. Tian, L. C. Murfin, L. Wu, S. E. Lewis and T. D. James, *Chem. Sci.*, 2021, **12**, 3406–3426.

82 W. Zhang, Z. Ma, L. Du and M. Li, *Analyst*, 2014, **139**, 2641–2649.

83 J. F. Callan, A. P. De Silva and D. C. Magri, *Tetrahedron*, 2005, **61**, 8551–8588.

84 H. S. Jung, P. Verwilst, W. Y. Kim and J. S. Kim, *Chem. Soc. Rev.*, 2016, **45**, 1242–1256.

85 P.-Y. Fu, B.-N. Li, Q.-S. Zhang, J.-T. Mo, S.-C. Wang, M. Pan and C.-Y. Su, *J. Am. Chem. Soc.*, 2022, **144**, 2726–2734.

86 A. C. Sedgwick, L. Wu, H.-H. Han, S. D. Bull, X.-P. He, T. D. James, J. L. Sessler, B. Z. Tang, H. Tian and J. Yoon, *Chem. Soc. Rev.*, 2018, **47**, 8842–8880.

87 A. W. Martinez, S. T. Phillips, G. M. Whitesides and E. Carrilho, *Diagnostics for the Developing World: Microfluidic Paper-Based Analytical Devices*, ACS Publications, 2010.

88 J. P. Devadhasan and J. Kim, *Sens. Actuators, B*, 2018, **273**, 18–24.

89 Y. Hang, J. Boryczka and N. Wu, *Chem. Soc. Rev.*, 2022, **51**, 329–375.

90 G. Hong, A. L. Antaris and H. Dai, *Nat. Biomed. Eng.*, 2017, **1**, 0010.

91 J. R. Choi, K. W. Yong, J. Y. Choi and A. C. Cowie, *Sensors*, 2019, **19**, 817.

92 A. Patti and D. Acierno, *Encyclopedia*, 2023, **3**, 665–676.

93 T. Yan, G. Zhang, H. Chai, L. Qu and X. Zhang, *Front. Bioeng. Biotechnol.*, 2021, **9**, 753692.

94 J. C. Stockert and A. Blázquez-Castro, *Fluorescence microscopy in life sciences*, Bentham Science Publishers, 2017.

95 M. S. Baranov, K. A. Lukyanov, A. O. Borissova, J. Shamir, D. Kosenkov, L. V. Slipchenko, L. M. Tolbert, I. V. Yampolsky and K. M. Solntsev, *J. Am. Chem. Soc.*, 2012, **134**, 6025–6032.

96 M. Ptaszek, *Prog. Mol. Biol. Transl. Sci*, 2013, **113**, 59–108.

97 E. Horak, M. Robić, A. Šimanović, V. Mandić, R. Vianello, M. Hranjec and I. M. Steinberg, *Dyes Pigm.*, 2019, **162**, 688–696.

98 X. Liu, B. Cho, L.-Y. Chan, W. L. Kwan and C.-L. K. Lee, *RSC Adv.*, 2015, **5**, 106868–106876.

99 Q. Zheng, M. F. Juette, S. Jockusch, M. R. Wasserman, Z. Zhou, R. B. Altman and S. C. Blanchard, *Chem. Soc. Rev.*, 2014, **43**, 1044–1056.

100 H. Lu, F. Su, Q. Mei, Y. Tian, W. Tian, R. H. Johnson and D. R. Meldrum, *J. Mater. Chem.*, 2012, **22**, 9890–9900.

101 H.-B. Cheng, Y. Li, B. Z. Tang and J. Yoon, *Chem. Soc. Rev.*, 2020, **49**, 21–31.

102 S. Xu, H.-W. Liu, S.-Y. Huan, L. Yuan and X.-B. Zhang, *Mater. Chem. Front.*, 2021, **5**, 1076–1089.

103 L. L. del Mercato, M. Moffa, R. Rinaldi and D. Pisignano, *Small*, 2015, **11**, 6417–6424.

104 I. L. Moldero, A. Chandra, M. Cavo, C. Mota, D. Kapsokalyvas, G. Gigli, L. Moroni and L. L. del Mercato, *Small*, 2020, 2002258.

105 R. Rizzo, V. Onesto, G. Morello, H. Iuele, F. Scalera, S. Forciniti, G. Gigli, A. Polini, F. Gervaso and L. L. del Mercato, *Mater. Today Bio*, 2023, **20**, 100655.

106 L. Hou, Y. Qin, J. Li, S. Qin, Y. Huang, T. Lin, L. Guo, F. Ye and S. Zhao, *Biosens. Bioelectron.*, 2019, **143**, 111605.

107 A. W. Martinez, S. T. Phillips, G. M. Whitesides and E. Carrilho, *Diagnostics for the Developing World: Microfluidic Paper-Based Analytical Devices*, ACS Publications, 2010.

108 J. Kaur and P. Singh, *Expert Opin. Ther. Pat.*, 2011, **21**, 437–454.

109 Z. Ma, G. Saluta, G. L. Kucera and U. Bierbach, *Bioorg. Med. Chem. Lett.*, 2008, **18**, 3799–3801.

110 J. Xu, G. Niu, X. Wei, M. Lan, L. Zeng, J. M. Kinsella and R. Sheng, *Dyes Pigm.*, 2017, **139**, 166–173.

111 A. Santoro, F. Tuyèras, G. Dupeyre, P. P. Laine, I. Ciofini, F. Nastasi, F. Puntoriero and S. Campagna, *Dyes Pigm.*, 2018, **159**, 619–636.

112 Y.-L. Tsai, C.-C. Chang, C.-C. Kang and T.-C. Chang, *J. Lumin.*, 2007, **127**, 41–47.

113 L. Xie, Y. Chen, W. Wu, H. Guo, J. Zhao and X. Yu, *Dyes Pigm.*, 2012, **92**, 1361–1369.

This journal is © The Royal Society of Chemistry 2026

J. Mater. Chem. C, 2026, **14**, 5607–5628 | **5625**

114 E. V. Antina, N. A. Bumagina, A. I. V'yugin and A. V. Solomonov, *Dyes Pigm.*, 2017, **136**, 368–381.

115 M. Mojzych and M. Henary, *Heterocyclic polymethine dyes: Synthesis, properties and applications*, 2008, pp. 1–9.

116 R. Irshad, S. Asim, A. Mansha and Y. Arooj, *J. Fluoresc.*, 2023, 1–31.

117 M. Homocianu and A. Airinei, *J. Fluoresc.*, 2016, **26**, 1617–1635.

118 V. Martinez and M. Henary, *Chem. – Eur. J.*, 2016, **22**, 13764–13782.

119 K. Ayyavoo and P. Velusamy, *New J. Chem.*, 2021, **45**, 10997–11017.

120 A. Chandra, S. Prasad, H. Iuele, F. Colella, R. Rizzo, E. D'Amone, G. Gigli and L. L. Del Mercato, *Chem. – Eur. J.*, 2021, **27**, 13318–13324.

121 W. Qiao and Z. Li, *Symmetry*, 2022, **14**, 966.

122 O. Karaman, G. A. Alkan, C. Kizilenis, C. C. Akgul and G. Gunbas, *Coord. Chem. Rev.*, 2023, **475**, 214841.

123 A. Chandra, S. Prasad, F. Alemanno, M. De Luca, R. Rizzo, R. Romano, G. Gigli, C. Bucci, A. Barra and L. L. Del Mercato, *ACS Appl. Mater. Interfaces*, 2022, **14**, 18133–18149.

124 R. Rizzo, V. Onesto, S. Forciniti, A. Chandra, S. Prasad, H. Iuele, F. Colella, G. Gigli and L. L. Del Mercato, *Biosens. Bioelectron.*, 2022, **212**, 114401.

125 D. Liu, Z. He, Y. Zhao, Y. Yang, W. Shi, X. Li and H. Ma, *J. Am. Chem. Soc.*, 2021, **143**, 17136–17143.

126 Q. Liu, Q. Sun, J. Shen, H. Li, Y. Zhang, W. Chen, S. Yu, X. Li and Y. Chen, *Coord. Chem. Rev.*, 2023, **482**, 215078.

127 W. Huang, L. U. O. Shenglin, Y. Dong and S. Zhang, *J. Zhejiang Univ. Sci. B*, 2021, **22**, 171.

128 A. Goncharov, H. Joung, R. Ghosh, G. Han, Z. S. Ballard, Q. Maloney, A. Bell, C. T. Z. Aung, O. B. Garner and D. Di Carlo, *Small*, 2023, 2300617.

129 Y. Cai, K. Kang, Q. Li, Y. Wang and X. He, *Molecules*, 2018, **23**, 1102.

130 Y. Sekine, S. B. Kim, Y. Zhang, A. J. Bandodkar, S. Xu, J. Choi, M. Irie, T. R. Ray, P. Kohli and N. Kozai, *Lab Chip*, 2018, **18**, 2178–2186.

131 P. Ghassemi, B. Wang, J. Wang, Q. Wang, Y. Chen and T. J. Pfefer, *IEEE Trans. Biomed. Eng.*, 2017, **64**, 1650–1653.

132 L. He, B. Chen, Y. Hu, B. Hu, Y. Li and X. Yang, *Anal. Bioanal. Chem.*, 2023, **415**, 5499–5509.

133 A. A. Alzu'bi, L. Zhou and V. J. M. Watzlaf, *Perspect. Health Inf. Manag.*, 2019, **16**, 1a.

134 B. H. Davis, G. DeFrank, N. A. Limdi and S. Harada, *Clin. Transl. Sci.*, 2020, **13**, 260–264.

135 R. C. Tseng, C.-C. Chen, S.-M. Hsu and H.-S. Chuang, *Sensors*, 2018, **18**, 2651.

136 A. K. Yetisen, N. Jiang, C. M. Castaneda Gonzalez, Z. I. Erenoglu, J. Dong, X. Dong, S. Stößer, M. Brischwein, H. Butt, M. F. Cordeiro, M. Jakobi, O. Hayden and A. W. Koch, *Adv. Mater.*, 2020, 1906762.

137 E. S. Kim, H. Chon, Y. Kwon, M. Lee, M. J. Kim and Y. H. Choe, *Ther. Drug Monit.*, 2024, **46**, 460–467.

138 J. Leonard, H. C. Koydemir, V. S. Koutnik, D. Tseng, A. Ozcan and S. K. Mohanty, *J. Hazard. Mater. Lett.*, 2022, **3**, 100052.

139 H. Kim, S.-K. Choi, J. Ahn, H. Yu, K. Min, C. Hong, I.-S. Shin, S. Lee, H. Lee, H. Im, J. Ko and E. Kim, *Sens. Actuators, B*, 2021, **329**, 129248.

140 M. Zhang, L. Gao, X. Zhao, Y. Duan, Y. Liao and T. Han, *Dyes Pigm.*, 2022, **205**, 110561.

141 Y. Lu, Z. Shi and Q. Liu, *Curr. Opin. Food Sci.*, 2019, **28**, 74–81.

142 G. Rateni, P. Dario and F. Cavallo, *Sensors*, 2017, **17**, 1453.

143 N. Cheng, Y. Song, M. M. A. Zeinhom, Y.-C. Chang, L. Sheng, H. Li, D. Du, L. Li, M.-J. Zhu, Y. Luo, W. Xu and Y. Lin, *ACS Appl. Mater. Interfaces*, 2017, **9**, 40671–40680.

144 Y. Shan, B. Wang, H. Huang, D. Jian, X. Wu, L. Xue, S. Wang and F. Liu, *Biosens. Bioelectron.*, 2019, **132**, 238–247.

145 N. C. Shaner, P. A. Steinbach and R. Y. Tsien, *Nat. Methods*, 2005, **2**, 905–909.

146 D. M. Chudakov, M. V. Matz, S. Lukyanov and K. A. Lukyanov, *Physiol. Rev.*, 2010, 1103.

147 S. J. Remington, *Protein Sci.*, 2011, 1509.

148 E. Balleza, J. M. Kim and P. Cluzel, *Nat. Methods*, 2018, **15**, 47–51.

149 A. Ibraheem and R. E. Campbell, *Curr. Opin. Chem. Biol.*, 2010, 30.

150 Z. Chen, T. M. Truong and H. W. Ai, *Chemosensors*, 2017, 32.

151 K. Horikawa, Y. Yamada, T. Matsuda, K. Kobayashi, M. Hashimoto, T. Matsu-ura, A. Miyawaki, T. Michikawa, K. Mikoshiba and T. Nagai, *Nat. Methods*, 2010, **7**, 729–732.

152 M. Deng, J. Yuan, H. Yang, X. Wu, X. Wei, Y. Du, G. Wong, Y. Tao, G. Liu, Z. Jin and J. Chu, *ACS Nano*, 2021, **15**, 17602–17612.

153 M. De, S. Rana, H. Akpinar, O. R. Miranda, R. R. Arvizo, U. H. F. Bunz and V. M. Rotello, *Nat. Chem.*, 2009, **1**, 461–465.

154 G.-T. Liang, C. Lai, Z. Yue, H. Zhang, D. Li, Z. Chen, X. Lu, L. Tao, F. V. Subach and K. D. Piatkevich, *Front. Bioeng. Biotechnol.*, 2022, 1039317.

155 M. Wang, L. Jin, P. Hang-Mei Leung, F. Wang-Ngai Chow, X. Zhao, H. Chen, W. Pan, H. Liu and S. Li, *Front. Bioeng. Biotechnol.*, 2024, 1393789.

156 F. R. Mansour, S. F. Hammad, I. A. Abdallah, A. Bedair, R. M. Abdelhameed and M. Locatelli, *TrAC, Trends Anal. Chem.*, 2024, **172**, 117596.

157 A. T. Krasley, E. Li, J. M. Galeana, C. Bulumulla, A. G. Beyene and G. S. Demirer, *Chem. Rev.*, 2024, **124**, 3085–3185.

158 L. N. Thwala, S. C. Ndlovu, K. T. Mpofu, M. Y. Lugongolo and P. Mthunzi-Kufa, *Nanomaterials*, 2023, **13**, 1247.

159 Y. Hang, A. Wang and N. Wu, *Chem. Soc. Rev.*, 2024, **53**, 2932–2971.

160 Q. Yang, Y. Wu, J. Chen, M. Lu, X. Wang, Z. Zhang, H. Xiong, J. Choo and L. Chen, *Coord. Chem. Rev.*, 2024, **507**, 215768.

161 M. Bartolomé, M. J. Villaseñor and Á. Ríos, *Anal. Chim. Acta*, 2025, 344693.

162 M. Jouyandeh, S. M. Sajadi, F. Seidi, S. Habibzadeh, M. T. Munir, O. Abida, S. Ahmadi, D. Kowalkowska-Zedler, N. Rabiee, M. Rabiee, G. Heidari, M. Hassanpour,

5626 | *J. Mater. Chem. C*, 2026, **14**, 5607–5628

This journal is © The Royal Society of Chemistry 2026

E. Nazarzadeh Zare and M. R. Saeb, *OpenNano*, 2022, **8**, 100104.

163 C. Jin, Z. Wu, J. H. Molinski, J. Zhou, Y. Ren and J. X. J. Zhang, *Mater. Today Bio*, 2022, **14**, 100263.

164 K. M. Ganesh, S. Bhaskar, V. S. K. Cheerala, P. Battampara, R. Reddy, S. C. Neelakantan, N. Reddy and S. S. Ramamurthy, *Nanomaterials*, 2024, **14**, 111.

165 M. Cedrún-Morales, M. Ceballos, E. Polo, P. del Pino and B. Pelaz, *Chem. Commun.*, 2023, **59**, 2869–2887.

166 M. Ceballos, S. Funes-Hernando, G. Zampini, M. Cedrún-Morales, J. M. Vila-Fungueiriño, B. Pelaz and P. del Pino, *Small Struct.*, 2024, 2300464.

167 M. Pamei and A. Puzari, *Nano-Struct. Nano-Objects*, 2019, **19**, 100364.

168 A. Kidanemariam and S. Cho, *Sensors*, 2025, **25**, 5081.

169 J. Zhang, Y. Li, F. Chai, Q. Li, D. Wang, L. Liu, B. Z. Tang and X. Jiang, *Sci. Adv.*, 2022, abo1874.

170 J. L. Vivero-Escoto, R. C. Huxford-Phillips and W. Lin, *Chem. Soc. Rev.*, 2012, **41**, 2673.

171 X. Ji, H. Wang, B. Song, B. Chu and Y. He, *Front. Chem.*, 2018, 38.

172 A. C. Siciliano, S. Forciniti, V. Onesto, H. Iuele, D. D. Cave, F. Carnevali, G. Gigli, E. Lonardo and L. L. del Mercato, *Adv. Healthcare Mater.*, 2024, 2401138.

173 R. Prieto-Montero, A. Katsumiti, M. P. Cajaraville, I. López-Arbeloa and V. Martínez-Martínez, *Sensors*, 2020, **20**, 5590.

174 H. Iuele, V. Onesto, A. C. Siciliano, S. Forciniti, F. Colella, G. Grasso, G. Gigli and L. L. del Mercato, *Chem. Eng. J.*, 2025, **525**, 170576.

175 F. Colella, S. Forciniti, V. Onesto, G. Grasso, H. Iuele, G. Gigli and L. L. del Mercato, *J. Mater. Chem. B*, 2024, **12**, 10573–10583.

176 S. Kakkar, P. Gupta, S. P. Singh Yadav, D. Raj, G. Singh, S. Chauhan, M. K. Mishra, E. Martín-Ortega, S. Chiussi and K. Kant, *Mater. Today Bio*, 2024, **28**, 101188.

177 S. Siavashy, M. Soltani, S. Rahimi, M. Hosseinali, Z. Guilandokht and K. Raahemifar, *Biosens. Bioelectron. X*, 2024, **19**, 100489.

178 V. Gubala, G. Giovannini, F. Kunc, M. P. Monopoli and C. J. Moore, *Cancer Nanotechnol.*, 2020, **11**, 1.

179 V. Secchi, A. Armanni, L. Barbieri, A. Bruno, A. Colombo, S. Fumagalli, E. A. Kukushkina, R. Lorenzi, L. Marchesi, H. Moukham, A. Paleari, A. Ronchi, G. Tomaino, F. Tripodi, M. Colombo, L. Sironi and A. Monguzzi, *Front. Nanotechnol.*, 2025, 1465429.

180 M. De Luca, M. M. Ferraro, R. Hartmann, P. Rivera-Gil, A. Klingl, M. Nazarenus, A. Ramirez, W. J. Parak, C. Bucci, R. Rinaldi and L. L. del Mercato, *ACS Appl. Mater. Interfaces*, 2015, **7**, 15052–15060.

181 L. Ouologuem, A. Kübler, S. Ouologuem, A. Hadzic, J. B. Stöckl, A. C. Siciliano, S. Forciniti, S. Nigro, H. Iuele, V. Onesto, A. Nguyen, D. Matzek, C. Abrahamian, C. Grimm, B. Popper, G. Gigli, L. L. del Mercato, O. M. Merkel, T. Fröhlich, S. Theurich and K. Bartel, *Front. Immunol.*, 2025, 1668066.

182 V. Onesto, S. Forciniti, F. Alemanno, K. Narayanankutty, A. Chandra, S. Prasad, A. Azzariti, G. Gigli, A. Barra, A. De Martino, D. De Martino and L. L. del Mercato, *ACS Nano*, 2023, **17**, 3313–3323.

183 F. Chen, G. Hableel, E. R. Zhao and J. V. Jokerst, *J. Colloid Interface Sci.*, 2018, **521**, 261–279.

184 S. Singh, A. Dhawan, S. Karhana, M. Bhat and A. K. Dinda, *Micromachines*, 2020, **11**, 1058.

185 V. G. Reshma and P. V. Mohanan, *J. Lumin.*, 2019, **205**, 287–298.

186 Z. Ramezani, F. K. Ghalehsardi and S. Noorizadeh, in *Quantum Dots in Bioanalytical Chemistry and Medicine*, Royal Society of Chemistry, 2023, pp. 1–36.

187 M. Nabil and F. Megahed, *J. Fluoresc.*, 2024, **34**, 2467–2484.

188 M. Ussia, V. Privitera and S. Scalese, *Adv. Mater. Interfaces*, 2024, 2300970.

189 G. Grasso, R. Scarfiello, F. Colella, V. Onesto, S. Forciniti, G. Gigli, L. Carbone and L. L. del Mercato, *Sens Actuators Rep.*, 2025, **9**, 100303.

190 Z. A. Qureshi, H. Dabash, D. Ponnamma and M. K. G. Abbas, *Heliyon*, 2024, **10**, e31634.

191 N. A. Pechnikova, K. Domvri, K. Porpodis, M. S. Istomina, A. V. Iaremenko and A. V. Yaremenko, *Aggregate*, 2025, e707.

192 M. Tavan, Z. Yousefian, Z. Bakhtiar, M. Rahmandoust and M. H. Mirjalili, *Ind. Crops Prod.*, 2025, **231**, 121207.

193 H. Tang, C. Lu, O. Kodra and J. Zhang, *Carbon Trends*, 2025, 100579.

194 T.-Q. Nguyen and A. Trentin, *Mater. Today Commun.*, 2025, **47**, 113204.

195 N. Sohal, S. Singla, S. J. Malode, S. Basu, B. Maity and N. P. Shetti, *ACS Appl. Nano Mater.*, 2023, **6**, 10925–10943.

196 H. Tavakoli, S. Mohammadi, X. Li, G. Fu and X. Li, *TrAC, Trends Anal. Chem.*, 2022, **157**, 116806.

197 J. Jin, J. Guo, J. Guo and D. Li, *Adv. Sens. Res.*, 2024, 2400037.

198 S. Wilhelm, *ACS Nano*, 2017, **11**, 10644–10653.

199 M. S. Arai and A. S. S. de Camargo, *Nanoscale Adv.*, 2021, **3**, 5135–5165.

200 J. Jin, Y.-J. Gu, C. W.-Y. Man, J. Cheng, Z. Xu, Y. Zhang, H. Wang, V. H.-Y. Lee, S. H. Cheng and W.-T. Wong, *ACS Nano*, 2011, **5**, 7838–7847.

201 K. S. Janbandhu, V. B. Pawade, A. M. Pethe and S. J. Dhoble, *Sci. Rep.*, 2025, **15**, 34517.

202 L.-D. Xu, F.-L. Du, J. Zhu and S.-N. Ding, *Analyst*, 2021, **146**, 706–713.

203 J. Guo, S. Chen, S. Tian, K. Liu, J. Ni, M. Zhao, Y. Kang, X. Ma and J. Guo, *Biosens. Bioelectron.*, 2021, **181**, 113160.

204 J. Hu, Y.-Z. Jiang, L.-L. Wu, Z. Wu, Y. Bi, G. Wong, X. Qiu, J. Chen, D.-W. Pang and Z.-L. Zhang, *Anal. Chem.*, 2017, **89**, 13105–13111.

205 L. Liang, M. Su, L. Li, F. Lan, G. Yang, S. Ge, J. Yu and X. Song, *Sens. Actuators, B*, 2016, **229**, 347–354.

206 A. M. Jimenez Jimenez, M. A. M. Rodrigo, V. Milosavljevic, S. Krizkova, P. Kopel, Z. Heger and V. Adam, *Sens. Actuators, B*, 2017, **240**, 503–510.

207 Y. F. Shi, Y. P. Jiang, X. Z. Wang, Z. Q. Zhang, J. Z. Huo, Y. Y. Liu, X. R. Wang and B. Ding, *ACS Appl. Nano Mater.*, 2022, **5**, 15629–15641.

This journal is © The Royal Society of Chemistry 2026

J. Mater. Chem. C, 2026, **14**, 5607–5628 | **5627**

208 J. Zou, X. Liu, X. Ren, L. Tan, C. Fu, Q. Wu, Z. Huang and X. Meng, *Nanoscale*, 2021, **13**, 7844–7850.

209 J. Zhang, Y. Zheng, J. Lee, A. Hoover, S. A. King, L. Chen, J. Zhao, Q. Lin, C. Yu, L. Zhu and X. Wu, *Adv. Sci.*, 2023, 2203943.

210 S. Tombelli, C. Trono, S. Berneschi, C. Berrettoni, A. Giannetti, R. Bernini, G. Persichetti, G. Testa, G. Orellana, F. Salis, S. Weber, P. B. Luppa, G. Porro, G. Quarto, M. Schubert, M. Berner, P. P. Freitas, S. Cardoso, F. Franco, V. Silverio, M. Lopez-Martinez, U. Hilbig, K. Freudenberger, G. Gauglitz, H. Becker, C. Gärtner, M. T. O'Connell and F. Baldini, *Anal. Bioanal. Chem.*, 2022, **414**, 3243–3255.

211 J. Zhang and G. Shi, *Anal. Chim. Acta*, 2022, 339572.

212 H. Liang, Y. Li, B. Lin, Y. Yu, Y. Wang, L. Zhang, Y. Cao and M. Guo, *Microchem. J.*, 2022, **175**, 107221.

213 B. Jin, Z. Li, G. Zhao, J. Ji, J. Chen, Y. Yang and R. Xu, *Anal. Chim. Acta*, 2022, **1192**, 339388.

214 Q. Zheng, M. F. Juette, S. Jockusch, M. R. Wasserman, Z. Zhou, R. B. Altman and S. C. Blanchard, *Chem. Soc. Rev.*, 2014, **43**, 1044–1056.

215 J. Liu, C. Liu and W. He, *Curr. Org. Chem.*, 2013, **17**, 564–579.

216 H.-B. Cheng, Y. Li, B. Z. Tang and J. Yoon, *Chem. Soc. Rev.*, 2020, **49**, 21–31.

217 B. C. Campbell, M. G. Paez-Segala, L. L. Looger, G. A. Petsko and C. F. Liu, *Nat. Methods*, 2022, **19**, 1612–1621.

218 J. K. Heppert, D. J. Dickinson, A. M. Pani, C. D. Higgins, A. Steward, J. Ahringer, J. R. Kuhn and B. Goldstein, *Mol. Biol. Cell*, 2016, **27**, 3385–3394.

219 D. Semeniak, D. F. Cruz, A. Chilkoti and M. H. Mikkelsen, *Adv. Mater.*, 2023, **35**, e2107986.

220 M. A. Farzin, S. M. Naghib and N. Rabiee, *TrAC, Trends Anal. Chem.*, 2025, **191**, 118345.

221 V. D. Punetha, P. Sanghani, M. Punetha and V. Pathak, *Upconversion Nanoparticles for Biomedical Applications*, Elsevier, 2026, pp. 1–43.

222 P. Navid, H. R. Akbari-Hasanjani and R. Akbari-Hasanjani, *Nano Select*, 2025, e70046.

223 J. K. Heppert, D. J. Dickinson, A. M. Pani, C. D. Higgins, A. Steward, J. Ahringer, J. R. Kuhn and B. Goldstein, *Mol. Biol. Cell*, 2016, **27**, 3385–3394.

224 D. Semeniak, D. F. Cruz, A. Chilkoti and M. H. Mikkelsen, *Adv. Mater.*, 2025, 2107986.

225 B. Liu, Y. Li, H. Wan, L. Wang, W. Xu, S. Zhu, Y. Liang, B. Zhang, J. Lou, H. Dai and K. Qian, *Adv. Funct. Mater.*, 2016, **26**, 7994–8002.

226 F. Zang, Z. Su, L. Zhou, K. Konduru, G. Kaplan and S. Y. Chou, *Adv. Mater.*, 2019, 1902331.

227 W. Hu, Z. Lu, Y. Liu, T. Chen, X. Zhou and C. M. Li, *Lab Chip*, 2013, **13**, 1797.

228 N. Yamaguchi, Y. Tokunaga, S. Goto, Y. Fujii, F. Banno and A. Edagawa, *Sci. Rep.*, 2017, **7**, 3092.

229 S. Shin, B. Kim, Y.-J. Kim and S. Choi, *Biosens. Bioelectron.*, 2019, **133**, 169–176.

230 Z. Göröcs, M. Tamamitsu, V. Bianco, P. Wolf, S. Roy, K. Shindo, K. Yanny, Y. Wu, H. C. Koydemir, Y. Rivenson and A. Ozcan, *Light Sci. Appl.*, 2018, **7**, 66.

231 H. Wang, Y. Rivenson, Y. Jin, Z. Wei, R. Gao, H. Günaydın, L. A. Bentolila, C. Kural and A. Ozcan, *Nat. Methods*, 2019, **16**, 103–110.

232 M. Wang, H. Liang, X. Chen, D. Chen, J. Wang, Y. Zhang and J. Chen, *Biosensors*, 2022, DOI: 10.3390/bios12070443.

233 H. Kanno, K. Hiramatsu, H. Mikami, A. Nakayashiki, S. Yamashita, A. Nagai, K. Okabe, F. Li, F. Yin, K. Tominaga, O. F. Bicer, R. Noma, B. Kiani, O. Efa, M. Büscher, T. Wazawa, M. Sonoshita, H. Shintaku, T. Nagai, S. Braun, J. P. Houston, S. Rashad, K. Niizuma and K. Goda, *Nat. Commun.*, 2024, **15**, 7376.

234 K. İçöz, A. Eken, S. Çınar, A. Murat, S. Özcan, E. Ünal and G. Deniz, *Sep. Sci. Technol.*, 2021, **56**, 2659–2666.

235 C. P. Y. Chan, W. C. Mak, K. Y. Cheung, K. K. Sin, C. M. Yu, T. H. Rainer and R. Renneberg, *Annu. Rev. Anal. Chem.*, 2013, **6**, 191–211.

236 M. Liu and Y. Wen, *Heliyon*, 2024, **10**, e38444.

237 S. Rasheed, T. Kanwal, N. Ahmad, B. Fatima, M. Najam-ul-Haq and D. Hussain, *TrAC, Trends Anal. Chem.*, 2024, **173**, 117640.

238 D. Strohmaier-Nguyen, C. Horn and A. J. Baeumner, *Biosens. Bioelectron.*, 2025, **267**, 116795.

239 G.-R. Han, A. Goncharov, M. Eryilmaz, S. Ye, B. Palanisamy, R. Ghosh, F. Lisi, E. Rogers, D. Guzman, D. Yigci, S. Tasoglu, D. Di Carlo, K. Goda, R. A. McKendry and A. Ozcan, *Nat. Commun.*, 2025, **16**, 3165.

240 T. Akkaş, M. Reshadsedghi, M. Şen, V. Kılıç and N. Horzum, *Adv. Mater.*, 2025, 2504796.

241 Y. Zhao, T. Sun, H. Zhang, W. Li, C. Lian, Y. Jiang, M. Qu, Z. Zhao, Y. Wang, Y. Sun, H. Duan, Y. Ren, P. Liu, X. Lang and S. Chen, *Biosensors*, 2025, **15**, 565.

242 R. W. Oei, G. Hou, F. Liu, J. Zhong, J. Zhang, Z. An, L. Xu and Y. Yang, *PLoS One*, 2019, **14**, e0213626.

243 A. Ait Lahcen, J. Rajendran and G. Slaughter, *Biosens. Bioelectron. X*, 2026, **28**, 100728.

244 H. Liu, E. Dai, R. Xiao, Z. Zhou, M. Zhang, Z. Bai, Y. Shao, K. Qi, J. Tu, C. Wang and S. Wang, *Sens. Actuators, B*, 2021, **329**, 129196.

245 F. Lin, C. Zhang, Z. Huang, Y. Wang, M. Yi, J. Li, X. Weng, Y. Chen, P. Lai and J. Qu, *Appl. Phys. Rev.*, 2026, 011303.

246 Y. Zu, H. Chang and Z. Cui, *Nexus*, 2025, **2**, 100059.

247 R. El-Khoury and G. Zaatari, *Diagnostics*, 2025, **15**, 2308.

5628 | *J. Mater. Chem. C*, 2026, **14**, 5607–5628

This journal is © The Royal Society of Chemistry 2026